A&A 495, 335–352 (2009)
DOI: 10.1051/0004-6361:200810105

Astronomy & Astrophysics

Extrasolar planets and brown dwarfs around A–F type stars⋆

VI. High precision RV survey of early type dwarfs with HARPS

A.-M. Lagrange[1], M. Desort[1], F. Galland[1], S. Udry[2], and M. Mayor[2]

[1] Laboratoire d'Astrophysique de l'Observatoire de Grenoble, Université Joseph Fourier, BP 53, 38041 Grenoble, France
e-mail: anne-marie.lagrange@obs.ujf-grenoble.fr
[2] Observatoire de Genève, 51 Ch. des Maillettes, 1290 Sauverny, Switzerland

Received 30 April 2008 / Accepted 10 October 2008

ABSTRACT

Aims. Systematic surveys to search for exoplanets have been mostly dedicated to solar-type stars sofar. We developed in 2004 a method to extend such searches to earlier A–F type dwarfs and started spectroscopic surveys to search for planets and quantify the detection limit achievable when taking the stars properties (Spectral Type, $v \sin i$) and their actual levels of intrinsic variations into account. We give here the first results of our southern survey with HARPS.
Methods. We observed 185 A–F ($B - V$ in the range $[-0.1; 0.6]$) stars with HARPS and analysed them with our dedicated software. We used several criteria to probe different origins for the radial-velocity variations – stellar activity (spots, pulsations) or companions: bisector shape, radial-velocity variations amplitudes, and timescales.
Results. 1) Sixty-four percent of the 170 stars with enough data points are found to be variable. Twenty are found to be binaries or candidate binaries (with stars or brown dwarfs). More than 80% of the latest type stars (once binaries are removed), are intrinsically variable at a 2 m s^{-1}precision level. Stars with earlier spectral type ($B - V \leq 0.2$) are either variable or associated to levels of uncertainties comparable to the RV rms observed on variable stars of the same $B - V$. 2) We detected one long-period planetary system (presented in another paper) around an F6IV–V star. 3) We quantified the jitter due to stellar activity and we show that when taking this jitter into account in addition to the stellar parameters (spectral type, $v \sin i$), it is still possible to detect planets with HARPS with periods of 3 days (resp. 10 days and 100 days) on 91% (resp. 83%, 61%) of them. We show that even the earliest spectral type stars are accessible to this type of search, provided they have a low projected rotational velocity and low levels of activity. 4) Taking the present data into account, we computed the actually achieved detection limits for 107 targets and discuss the limits as a function of $B - V$. Given the data at hand, our survey is sensitive to short-period (few days) planets and to longer ones (100 days) to a lower extent (latest type stars). We derive first constrains on the presence of planets around A–F stars for these ranges of periods.

Key words. techniques: radial velocities – stars: early-type – stars: planetary systems – stars: variables: general

1. Introduction

Since the discovery of the first exoplanet around a solar-like star in 1995, more than 250 planets have been found by radial-velocity (RV) surveys (Jean Schneider, http://exoplanet.eu). These surveys have generally focused on late-type stars (later than F8). However, knowing about the presence of planets or brown dwarfs (hereafter BDs) around more massive objects is mandatory if one wishes to investigate the impact of the mass of the central stars on the planetary formation and evolution processes.

There are theoretical indications that the mass of the planets increases with the mass of the parent star, at least for low-mass stars (Ida & Lin 2005) and that the frequency of giant planets increases linearly with the parent-star mass for stars between 0.4 and 3 $M_\odot$ (Kennedy & Kenyon 2008), with e.g., 6% frequency of giant planets around 1 $M_\odot$ and 10% frequency around 1.5 $M_\odot$. More numerous and massive planets are consistent with what we could expect from a disk surface-density increasing with stellar mass. On the other hand, the shorter lifetimes of the systems, as well as the lack of solid material close to the star, could reduce the number of planets. Clearly, several parameters probably impact the occurrence and properties of planets around massive stars, and they have not been fully explored yet.

The data to test the models are still quite limited, as the largest and earliest, now long-lasting surveys have focused on solar type, main-sequence (MS) stars. In recent years, some efforts have been made nevertheless to search for planets around stars with various masses: less massive, M-type stars, on the one hand, and more massive stars, on the other. The search for planets around M stars so far seems to confirm the previously mentioned expectations from theoretical works (see e.g., Bonfils et al. 2005; Butler et al. 2006). The available observations of massive stars are still very limited. Massive MS stars have been removed from early surveys, because it was generally thought that their spectra (few lines, usually broadened by stellar rotation) would not allow planet detection and, indeed, the classical RV measurements technique (based on the cross correlation of the actual spectra with a binary spectral mask corresponding to a star with an appropriate spectral type and $v \sin i = 0$ km s^{-1}) fail to measure the RV of these stars. This has led some groups to study "retired" early-type instead, either low-mass ($\leq$1.6 $M_\odot$) giants, intermediate-mass (1.6–2 $M_\odot$) subgiants, or clump giants (1.7–3.9 $M_\odot$) (see e.g., Hatzes et al. 2005; Niedzielski et al. 2007; Johnson et al. 2006, 2007; Lovis & Mayor 2007;

⋆ Based on observations collected at the European Southern Observatory, Chile, ESO 075.C-0689, 076.C-0279, 077.C-0295, 078.C-0209, 080.C-0664, 080.C-0712.

Sato et al. 2008). These stars have indeed cooled down and also rotate more slowly due to coupling of stellar winds and magnetic fields. They therefore exhibit more numerous, narrower lines, which is adequate for classical RV measurements technique, and their level of activity (jitter) is relatively low (10–20 $m\,s^{-1}$, Hekker et al. 2006) for giants and 10 $m\,s^{-1}$ for subgiants (Johnson et al. 2007, and ref. therein; Sato et al. 2008). The data available today are still more limited than for solar-type stars, and less than 20 planets have been found so far in total around these evolved stars. So far, the planets found around K subgiants stars with $M \geq 1.5\ M_{\odot}$ are located at distances greater than 0.8 AU (Johnson et al. 2007), which has led these authors to conclude that close-in planets are rare, in agreement with some theoretical predictions on disk depletion timescales (Burkert & Ida 2007). However, the impact of the post MS evolution of the stars on closer-in planets has not been explored yet for these stars. All planets found so far around giant stars have relatively long periods, the closest ones being reported at less than 0.7 AU from 2 giants, in addition to a previously reported planet at 0.7 AU by Sato et al. (2003). Numerical simulations by the same authors suggest that planets with orbits inside 0.5–1 AU around 2–3 $M_{\odot}$ stars could be engulfed by the central stars at the tip of RGB thanks to tidal torque from the central stars. According to them, if one then assumes that most of the clump giants are post RGB stars, there is then a risk that closer planets, if present before, had disappeared as the star evolved. In summary, even though there are some hints that hot Jupiters are not present around retired stars, it is recognized that data are still needed to definitely confirm this point. Also, because stellar evolutionary processes may have affected the presence of planets close to the stars, it is acknowledged that data are needed on A–F MS stars (see e.g., Burkert & Ida 2007; see also Li et al. 2008). We note finally that short-period planets have indeed been found around F5–F6 MS stars through transit observations (see http://exoplanet.eu).

A few years ago we developed a software dedicated to extracting the RV data around early type MS stars. The method consists in correlating, in the Fourier space, each spectrum and a reference spectrum built by summing-up all the available spectra for this star. We had shown earlier that with this approach and by taking the stars $B - V$ and projected rotational velocities into account, it is possible to find planets around A–F type stars (Galland et al. 2005a). However, the price to pay is that more measurements are needed to find planets around A and early F dwarfs than for late F and G–K dwarfs, because of the relatively higher uncertainties in the RV measurements due to higher $v \sin i$ and higher effective temperature, and also because of the possible presence of pulsations or spots in the case of late F stars, the impact of which has not been quantified so far. (Spots or pulsations become also a limiting factor in the case of later-type stars, as well as pulsations, if one looks for low mass planets.) We then started systematic searches for low-mass companions to A–F type stars, with HARPS in the southern hemisphere and with ELODIE and then SOPHIE at OHP in the northern hemisphere. We have so far found a 9.1 $M_{\rm Jup}$ (minimum mass) planet orbiting (a = 1.1 AU) an F6V star, with $v \sin i$ = 12 $km\,s^{-1}$ (Galland et al. 2005b). Very promisingly, we also detected a 21 $M_{\rm Jup}$ brown dwarf orbiting (a = 0.2 AU) a pulsating A9V star with $v \sin i$ = 50 $km\,s^{-1}$ (Galland et al. 2006); noticeably, in that case, we could disentangle stellar pulsations from the presence of a low-mass companion.

In parallel, we developed detailed simulations of stellar activity (spots) in order to estimate more quantitatively than what was available so far (Saar & Donahue 1997; Hatzes 2002) the impact of such stellar activity on RV data and other observables (bisectors, bisectors velocity-span, photometry). We showed that if the star $v \sin i$ is smaller than the spectrograph spectral resolution, depending on their location with respect to the line of sight, depending on their size, spots with realistic sizes can produce RV variations and bisector velocity-span variations that are quite similar to those of low-mass planets. Hence, low amplitude (level of typically 20 $m\,s^{-1}$ or less) planetary-like RV and bisector velocity span variations alone cannot definitely prove the presence of planets around low $v \sin i$ G–K stars (Desort et al. 2007), so additional criteria are mandatory for ruling out spots: photometry, activity evaluation down to levels relevent to explain the amplitude of RV variations, precise knowledge of the star rotaional period, etc. That situation is much more favorable in the case of earlier-type stars because they rotate statistically faster, so the bisector criteria can apply.

The present paper is devoted to our southern hemisphere survey. The sample, observations, measurements, and diagnostics are provided in Sect. 2. The results concerning the stellar variability and the quantitative impact on planet detectability around the early-type stars are presented in Sect. 3. Finally we give and discuss the detection limits obtained in the present survey in Sect. 4.

2. Sample, observations, and measurements

2.1. Sample

Our HARPS sample is limited to B8 to F7 dwarfs. The limit in spectral type (ST) at F7 is set because the surveys using the masking technique generally start with stars with ST later than F8. The limit at B8 is set by the precision that can be obtained with our method on stars, given their ST and their $v \sin i$ (Galland et al. 2005a): the detection limit of stars with ST earlier than B8 does not fall into the planet domain. Our survey is also volume-limited with an upper limit at 67 pc for the B8–A9 dwarfs and at 33 pc for the F0–F7 dwarfs. The distance was taken from Hipparcos catalog, and stars with distance uncertainties over 20% were removed. The difference in distance for both spectral types comes from our wanting to have roughly the same number of A and F stars. The dwarf nature was selected by selecting stars with absolute magnitudes within 2.5 mag from the main sequence.

Spectroscopic binaries and close visual binaries with separations smaller than 5″ known at the beginning of the survey from Coravel or Hipparcos data were removed. Confirmed δ Scuti (from Rodriguez et al. 2000) and γ Doradus type stars (from Mathias et al. 2004 and http://astro.univie.ac.at/dsn/gerald/gdorlist.html) were also removed because they are known to produce RV variations over hours to a few days due to pulsations. Finally we also removed Ap and Am stars, which present spectral anomalies and are often associated to binary systems. This removes a number of late A – early F type stars, crossing the δ Scuti and γ Doradus instability strip. We ended up with 207 stars with ST between B8 and F7, and $B - V$ respectively ranging between −0.1 and 0.58, corresponding to mass ranging between 1.3 and 3.5 $M_{\odot}$. We have a relatively smaller number of stars in the [0.2; 0.4] $B - V$ range (i.e., roughly, between 1.8 and 1.4 $M_{\odot}$) as we removed the known δ Scuti and γ Doradus stars).

2.2. Observations

In all, 185 stars have been observed between August 2005 and January 2008. Figure 1 shows their position in the HR diagram.

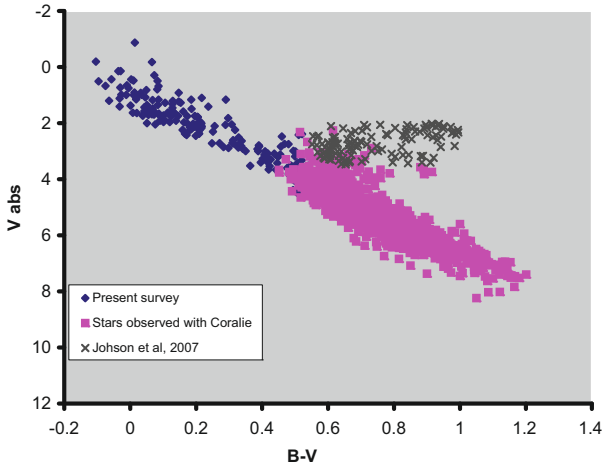

Fig. 1. Observed stars in an HR diagram. We also plotted the dwarfs and/or (sub-) giants surveyed either with the Coralie spectrograph or by Johnson et al. (2006). Our targets cover a domain that has not been surveyed yet. Note the relative lack of objects in the [0.2; 0.4] $B-V$ region, due to selection effects (see text).

It can be seen that our survey fills a domain of the HR diagram that has not been covered yet.

We usually recorded 2 consecutive high-resolution ($R \simeq 115\,000$) spectra each time we pointed to the star (each pointing is hereafter referred to as one epoch). The spectra cover a wavelength range between 3800 and 6900 Å. As far as possible, we tried to record data at two or three different times for a given object during one night, in order to identify possible high-frequency RV variations. We also tried whenever possible to record data on two or three consecutive nights. The time baseline for a given star varies between 5 days and more than 800 days. Only a few (11) stars have been observed during one night only, but for 15 stars we only got 4 good quality spectra or less (i.e., with a magnitude difference[1] between the observation and the one that gives the best signal-to-noise ratio (SN) smaller than 2). We ended up with 170 dwarfs for which we recorded 6 or more good quality spectra. 45 have $B-V \leq 0.1$; 72 have $B-V$ between 0.1 and 0.4 and 53 have $B-V \geq 0.4$. We hereafter limit our study to those stars.

Typical exposure times ranged between 30 s and 15 min depending on the star magnitude and on the atmospheric conditions. Table 1 provides the 170 targets observed, together with several relevant pieces of information on the stars (ST, $v \sin i$, $B-V$) and on the data obtained, as well as various measurements (see below).

2.3. Measurements

2.3.1. Radial velocities

The extraction of the radial velocities is fully described in Galland et al. (2005a). Briefly, for each star, we built a first estimate of the reference spectrum that is the average of the spectra recorded and reduced via the STS HARPS pipeline. We then computed a first estimate of the RV for each spectrum, by correlating each spectrum and this first estimate of the reference spectrum in Fourier space. We then built a final reference spectrum by averaging the spectra once they had been shifted from their measured RV. For each spectrum we finally measured the RV velocity with respect to this reference spectrum. We also measured the uncertainties associated to each RV measurement.

To build up the reference we computed the χ^2 of each spectrum compared to the first estimate of the reference spectrum. Most of the time, the χ^2 found was much less than 10. Whenever a higher χ^2 was found, we checked the spectra. In such cases, either they were due to bad observing conditions or technical problems and were not kept to build the reference spectrum (this actually happened quite rarely as we already selected spectra with acceptable absorptions) or they were associated to line deformations indicative of a type-2 binary.

2.3.2. CCFs, bisectors and bisectors velocity-span

Whenever possible (see below), we computed the resulting cross-correlation functions (CCFs) and the bisector's velocity-span for each target (see for their definition Galland et al. 2005a). Indeed, the bisector and bisectors' velocity span are very good diagnostics of stellar activity (spots, pulsations) provided 1) they can be measured (see below), and 2) the star projected rotational velocity is higher than the instrumental resolution (see Desort et al. 2007).

The uncertainty associated to the bisectors' velocity span depends directly on the projected rotational-velocity and/or their spectra type. Indeed, the number of lines used to compute the CCF depends on these two parameters (much more than on the signal-to-noise ratio). For stars with high $v \sin i$ (typ. ≥ 150 km s^{-1}) and/or $B-V \leq 0.1$, the number of lines may be quite low (30–50) whereas for late-type stars with moderate $v \sin i$ (10–20 km s^{-1}), the number of lines used is a few hundreds (up to about 1000). When the bisectors had been computed, we then attributed quality flags to the bisectors' velocity-span measurements, respectively: Good, Acceptable, Bad, corresponding to numbers of lines respectively ≥100, 40–100, and ≤40.

2.4. Diagnostics for the classification of variable stars

Variable stars are defined as having an RV standard deviation (rms) more than twice the RV uncertainties and a total RV amplitude more than 6 times the RV uncertainties. The RV variations can a priori be due to the presence of a companion (star, brown dwarf, planet) or to intrinsic variations of the star (spots, pulsations). It can also be a combination of those different origins.

2.4.1. Binarity

We first checked those stars with high χ^2 (≥10) and looked for line deformations indicative of spectroscopic binaries. Figure 2 provides an example of a binary SB2 identified on the basis of the χ^2, HD 2885 (A2V; $v \sin i = 40$ km s^{-1}). It has to be noted that, in such cases, the RV values measured are no longer valid, as our RV extraction method assumes that all lines in a given spectrum originate from the same object.

For the rest of the variable stars, we tried to identify binary stars among the stars for which the RV amplitude can be explained by the presence of a stellar or BD companion. To do so, using rough estimations of the star masses via their $B-V$, we computed the RV amplitude $2 \times K_{2d}$ expected from the presence of a 13 M_{Jup} body orbiting with a period of 2 days and the

[1] $\Delta m(i) = 6 \log_{10}[\epsilon_{rv}(i)/\min(\epsilon_{rv})]$, where $\epsilon_{rv}(i)$ stands for the uncertainty associated to the measurement of the observation (i) for the considered object, and $\min(\epsilon_{rv})$ is the lowest value of uncertainty obtained for this object; the measured uncertainties (cf. Galland et al. 2005a) take the photon noise + instrumental uncertainties into account.

Table 1. Stars properties and measurements.

HD	ST	$B-V$	$v \sin i$ ($km\,s^{-1}$)	Time bs l (days)	RV rms ($m\,s^{-1}$)	RV unc ($m\,s^{-1}$)	RV ampl ($m\,s^{-1}$)	Span rms ($m\,s^{-1}$)	Span unc ($m\,s^{-1}$)	Span ampl ($m\,s^{-1}$)	Bis. Flag	Variabl.	Bin.
HD 693	F5V	0.487	10	389.1	2	1	6	2	1	7	G	V	
HD 2696	A3V	0.128	150	389.1	279	166	847					C	
HD 2834	A0V	0.018	130	279.2	9408	164	29717					V	V
HD 2884	B9V	-0.06	170	603.2	587	496	2141					C	
HD 2885	A2V	0.147	40	820.7	9331	19	34510				B	V	X
HD 3003	A0V	0.038	115	603.2	135	83	491					C	
HD 4247	F0V	0.35	35	842.8	26	11	94	62	49	216	G	V	
HD 4293	A7V	0.297	125	837.8	91	99	270	4109	1281	16151	B	C	
HD 7439	F5V	0.448	8	453.8	10	1	22	24	2	63	G	V	
HD 9672	A1V	0.066	195	453.8	169	300	527					C	
HD 11262	F6V	0.523	5	840.8	2500	1	5014	30	2	64	G	V	B
HD 12311	F0V	0.29	22	387.9	3674	80	10137	3113	757	12217	G	V	B
HD 13555	F5V	0.457	9	821.8	13	1	42	20	3	54	G	V	
HD 14943	A5V	0.213	111.5	835.8	141	50	667	745	484	6364	A?	V	
HD 15008	A3V	0.034	180	1165.9	367	274	1210					C	
HD 17848	A2V	0.101	220	842.8	294	194	1046					C	
HD 18978	A4V	0.163	120	1161.8	185	88	880	13988	1317	105268	B	V	
HD 19107	A8V	0.193	170	389	154	176	434					C	
HD 19545	A3V	0.166	80	821.9	1490	33	3962	623	244	2389	A	V	B
HD 21882	A5V	0.205	255	382.9	400	350	1332					C	
HD 25457	F5V	0.516	25	368.1	28	3	93	28	8	82	G	V	
HD 25490	A1V	0.032	65	5	74	71	214					C	
HD 29488	A5V	0.147	115	665.2	183	72	712	3160	855	23124	B	V	
HD 29875	F2V	0.342	45	325	434	7	1100	1108	36	2551	G	V	
HD 29992	F3V	0.391	100	638.2	335	30	855	319	226	1386	G	V	
HD 30652	F6V	0.484	16	500.7	13	2	54	19	7	90	G	V	
HD 30739	A1V	0.01	195	328	941	631	3380					C	
HD 31746	F3V	0.442	11.4	295	18	2	60	45	6	144	G	V	
HD 32743	F2V	0.421	50	663.2	13	5	44	145	42	441	A	V	
HD 32977	A5V	0.118	100	175.7	70	47	279	272	340	990	A/B	C	
HD 33256	F2V	0.455	10	326	4	2	14	5	4	16	G	V	
HD 33262	F7V	0.526	30	665.1	17	3	45	60	7	173	G	V	
HD 37306	A2V	0.051	130	670.2	275	180	1127					C	
HD 38393	F7V	0.481	8.4	1165.9	4	1	19	5	2	22	G	V	
HD 38678	A2V	0.104	200	338.1	723	429	1942					C	
HD 39014	A7V	0.217	205	665.2	512	173	2376					V	
HD 39060	A3V	0.171	130	670.1	287	39	996	883	423	3702	A	V	
HD 40136	F1V	0.337	18	663.2	10	3	36	19	7	77	G	V	
HD 41695	A0V	0.046	250	280.2	595	628	2046					C	
HD 41742	F4V	0.493	26.3	450.9	673	5	2030	44	17	148	G	V	B
HD 43940	A2V	0.139	247.5	282.2	597	513	1939					C	
HD 46089	A3V	0.185	110	0.1	1060	64	2618	3148	687	8811	A	V	
HD 49095	F7V	0.491	7	337.9	3	1	13	4	2	21	G	V	
HD 49933	F2V	0.396	12	29	29	2	85	83	4	237	G	V	
HD 50445	A3V	0.183	90.7	670.1	66	36	248	301	295	1672	A	C	
HD 54834	A9V	0.312	26.9	0.9	1183	11	2839	127	657	312	G	V	B
HD 56537	A3V	0.106	140	666.2	180	75	639	3198	1090	15172	A	V	
HD 59984	F5V	0.54	15	29.9	3	1	10	30	24	107	B	V	
HD 60532	F6V	0.521	10	667	26	1	109	4	2	22	G	V	
HD 60584	F6V	0.468	38.9	663.1	23	9	83	62	44	215	G	V	
HD 63847	A9V	0.31	94	339	794	65	3145	997	565	3835	A	V	
HD 66664	A1V	0.018	175	32.8	542	450	1695	0	0	0		C	
HD 68146	F7V	0.488	8	666.1	4	1	16	5	3	27	G	V	
HD 68456	F5V	0.437	12	212.3	1236	2	3613	70	4	177	G	V	B
HD 71155	A0V	-0.012	115	337.9	480	227	2288					V	
HD 73262	A1V	0.003	265	30.9	1101	777	3843					C	
HD 74591	A6V	0.2	115	338	171	80	639	726	901	3137	B	V	
HD 74873	A1V	0.12	10	28.9	1534	114	5167	0	0	0		V	
HD 75171	A9V	0.217	93.3	388	294	57	934	713	443	2021	A	V	
HD 76653	F6V	0.481	11	282.1	13	1	45	14	3	55	G	V	

Table 1. continued.

HD	ST	$B-V$	$v \sin i$ (km s^{-1})	Time bs l (days)	RV rms (m s^{-1})	RV unc (m s^{-1})	RV ampl (m s^{-1})	Span rms (m s^{-1})	Span unc (m s^{-1})	Span ampl (m s^{-1})	Bis. Flag	Variabl.	Bin.
HD 77370	F3V	0.417	95	667.1	37	15	134	136	71	504	G	V	
HD 82165	A6V	0.216	232.8	32	541	276	2046					C	
HD 83446	A5V	0.173	155	670.1	274	83	1152					V	
HD 88955	A2V	0.051	105	99.8	115	69	450					C	
HD 89328	A8V	0.329	302.8	568.3	340	93	956					V	
HD 90132	A8V	0.251	270	28.9	433	221	1647					C	
HD 91324	F6V	0.5	8	665.1	3	1	13	6	3	25	G	V	
HD 91889	F7V	0.528	6	665	4	1	17	2	1	9	G	V	
HD 93372	F6V	0.51	11.3	638.1	4	2	14	8	5	28	G	C	
HD 94388	F6V	0.48	8	31.9	15	1	51	27	3	79	G	V	
HD 96819	A1V	0.069	230	5	463	442	1520					C	
HD 97244	A5V	0.209	75	106.8	84	45	298	301	360	1246	A	C	
HD 97603	A4V	0.128	165	32.9	315	170	987	0	0	0		C	
HD 99211	A9V	0.216	130	29.9	135	59	474	433	592	1796	A	V	
HD 99453	F7V	0.495	5	32	253	1	784					V	X
HD 100563	F5V	0.48	14	564.3	3	2	10	12	4	35	G	C	
HD 101198	F7V	0.52	5	662.1	40	1	102	2	1	5	G	V	
HD 102124	A4V	0.174	130	29.9	297	114	1195	2230	1928	7132	B	V	
HD 102647	A3V	0.09	115	106.8	111	44	426	419	454	2305	A	V	
HD 104731	F6V	0.417	20	29.9	23	2	75	129	6	445	G	V	
HD 105850	A1V	0.055	122	569.3	181	107	606					C	
HD 106661	A3V	0.068	175	32	358	373	1272					C	
HD 109085	F2V	0.388	81	638	22	15	77	86	82	329	G	C	
HD 109787	A2V	0.049	330	32.9	829	509	3038					C	
HD 110411	A0V	0.076	140	32.9	851	415	2748					V	
HD 111998	F5V	0.493	28.5	638.1	40	5	144	35	18	128	G	V	
HD 112934	A9V	0.298	70	73.8	857	43	2877	580	289	1950	G	V	B
HD 114642	F6V	0.46	13	105.7	49	2	194	118	4	448	G	V	
HD 115892	A2V	0.068	90	101.8	59	29	232					V	
HD 116160	A2V	0.045	205	97.7	4080	437	10844					V	V
HD 116568	F3V	0.415	40	74.9	1243	8	2751	154	36	592	G	V	B
HD 118098	A3V	0.114	205	105.9	395	263	1533					C	
HD 124850	F7V	0.511	15	5	39	2	129	88	6	278	G	V	
HD 125276	F7V	0.518	5	182.8	1	1	4	2	1	8	G	C	
HD 126248	A5V	0.124	185	280.2	602	204	2482					V	
HD 128020	F7V	0.506	5	73.8	2	1	6	3	2	10	G	C	
HD 128167	F3V	0.364	8	6	21	3	70	56	5	169	G	V	
HD 128898	F1V	0.256	15	0.1	64	2	189	41	6	121	G	V	
HD 129422	A7V	0.308	200	113.9	562	196	1742					V	
HD 129926	F0V	0.315	110	73.9	347	26	1074	642	214	2358	G	V	
HD 130109	A0V	-0.005	265	31	1319	945	4253					C	
HD 132052	F0V	0.318	105	182.6	139	31	496	495	253	1490	G	V	
HD 133469	F6V	0.489	24.3	182.6	17	5	60	32	17	104	G	V	
HD 135379	A3V	0.088	60	841.8	31	22	105	109	153	435	G	C	
HD 135559	A4V	0.181	125	389	505	87	2063	1626	1166	6894	B	V	
HD 138763	F7V	0.577	7	623.2	56	2	200	54	4	217	G	V	
HD 139211	F6V	0.505	7	182.7	3	1	12	3	2	12	G	V	
HD 141513	A0V	-0.036	85	389	147	55	599					V	
HD 141851	A3V	0.135	185	114.9	604	482	1899					C	
HD 142139	A3V	0.087	110	5	45	45	142	234	327	681	A	C	
HD 142629	A3V	0.129	85	386.9	2207	25	6526				G	V	X
HD 145689	A4V	0.159	100	112.9	198	62	604	807	618	2460	B	V	
HD 146514	A9V	0.326	145	389	820	134	2368	2559	1861	7544	B	V	
HD 146624	A0V	0.008	30	724.9	10	15	33	51	57	167	G	C	
HD 147449	F0V	0.338	83	389	65	19	265	216	127	996	G	V	
HD 153363	F3V	0.407	27	279.2	204	10	590	236	41	637	G	V	
HD 156751	A5V	0.248	93.8	5.9	474	80	1359	1281	607	3866	B	V	
HD 158094	B8V	-0.104	255	386	1876	539	5639					V	V
HD 158352	A8V	0.237	165	388	1399	90	3968					V	V

Table 1. continued.

HD	ST	$B-V$	$v \sin i$ ($km\,s^{-1}$)	Time bs l (days)	RV rms ($m\,s^{-1}$)	RV unc ($m\,s^{-1}$)	RV ampl ($m\,s^{-1}$)	Span rms ($m\,s^{-1}$)	Span unc ($m\,s^{-1}$)	Span ampl ($m\,s^{-1}$)	Bis. Flag	Variabl.	Bin.
HD 159170	A5V	0.187	225	114.8	636	344	2541					C	
HD 159492	A7V	0.195	60	446.9	106	20	371	429	108	1333	G	V	
HD 160613	A2V	0.086	95	389	98	61	323					C	
HD 161868	A0V	0.043	185	388.1	772	763	2860					C	
HD 164259	F3V	0.39	80	833.9	66	18	190	198	113	651	G	V	
HD 167468	A0V	0.043	295	278.2	968	482	3371					V	
HD 171834	F3V	0.386	60	388.1	22	19	69	170	125	612	G	C	
HD 172555	A7V	0.199	175	841.8	256	62	1165					V	
HD 175638	A5V	0.161	145	389.1	191	77	942	180186	1019	1247939	B	V	
HD 175639	A5V	0.204	200	110.8	735	257	2033					V	
HD 176638	A0V	-0.021	260.8	278.3	1998	1287	5542					C	
HD 177178	A4V	0.182	155	280.3	546	187	1932					V	
HD 177724	A0V	0.014	295	833.9	2752	1399	9102					C	
HD 177756	B9V	-0.096	160	833.8	5101	555	17662					V	V
HD 181296	A0V	0.02	420	1283.8	1559	905	6283					C	
HD 184985	F7V	0.501	5	389.1	3	1	13	2	1	7	G	V	
HD 186543	A9V	0.196	121.5	837	150	53	614	2137	583	15115	B	V	
HD 187532	F0V	0.402	95	829.9	33	21	133	240	143	974	G	C	
HD 188228	A0V	-0.032	115	841.9	117	90	450					C	
HD 189245	F7V	0.498	100	259.1	86	17	267	137	109	503	G	V	
HD 191862	F5V	0.476	8	364.2	3	2	12	9	4	31	G	C	
HD 196385	A9V	0.328	13	568.7	12	5	44	19	12	84	G	V	
HD 197692	F5V	0.426	40	829.9	30	7	118	85	33	307	G	V	
HD 198390	F5V	0.42	6.5	389.1	3	2	9	6	3	18	G	C	
HD 199254	A4V	0.131	145	368	178	93	637	2678	1270	10547	B	C	
HD 199260	F7V	0.507	13	829.9	13	2	50	22	6	74	G	V	
HD 200761	A1V	-0.01	80	841.8	2095	107	5619					V	V
HD 202730	A5V	0.191	210	366.9	107	86	387					C	
HD 203608	F6V	0.494	8	909.8	2	1	6	2	1	9	G	V	
HD 205289	F5V	0.423	45	829.9	29	14	94	62	81	208	G	C	
HD 209819	B8V	-0.075	135	387.9	8182	220	21581					V	X
HD 210302	F6V	0.489	12	1287.7	9	2	38	10	4	40	G	V	
HD 210418	A2V	0.086	130	836.8	298	144	971					V	
HD 210739	A3V	0.169	160	837.9	375	307	1365					C	
HD 211976	F6V	0.451	5	368	4	2	11	4	3	16	G	V	
HD 212728	A3V	0.208	254.9	1165.9	749	501	2351					C	
HD 213398	A1V	0.011	45	1161.9	38	24	124	60	50	208	G	C	
HD 213845	F7V	0.446	25	841.8	26	6	99	40	25	156	G	V	
HD 215789	A3V	0.083	270	719	241	306	807					C	
HD 216627	A3V	0.066	70	389.2	4058	35	9514	154	274	519	G	V	B
HD 216956	A3V	0.145	85	325.2	52	17	282	277	150	1256	G	V	
HD 219482	F7V	0.521	7	837.9	14	2	38	10	3	36	G	V	
HD 220729	F4V	0.409	20	386	8018	4	19021	6428	10	14987	G	V	B
HD 222095	A2V	0.082	165	387	200	109	741					C	
HD 222368	F7V	0.507	7	837.8	3	1	12	2	2	12	G	V	
HD 222603	A7V	0.2	60	385.1	296	20	765	573	98	1442	G	V	
HD 222661	B9V	-0.032	135	388.1	348	239	1031					C	
HD 223011	A7V	0.21	35.3	840.9	364	13	1177	282	63	1056	G	V	
HD 223352	A0V	0.001	280	708.1	1643	1453	4917					C	
HD 223781	A4V	0.186	165	368	365	335	1148					C	
HD 224392	A1V	0.06	250	385.9	325	383	944					C	

"RV rms" (resp. "span rms") stands for the rms of the measured radial velocities (resp. bisector velocity-spans); "RV amp" (resp. "Span amp.") stands for amplitude of the measured radial velocities (resp. bisector velocity-spans); "RV unc." (resp. "Span unc.") stands for the average uncertainties associated to the RV (resp. bisector velocity-spans) data. Bisector flags: G: good quality; B: bad quality; A: acceptable quality. Binary types: X refers to stars identified as binaries based on a high χ^2 ($\geq$10); B refers to binaries identified via a flat or a composite bisector, and V refers to stars regarded as binary candidates, based on the sole amplitude of their RV variations (see text).

RV amplitude $2 \times K_{200d}$ expected in the case of a 200-day period and compared these quantities to the observed RV amplitudes, once corrected from the RV variations observed within a night (in practice, over a few hours), as the variations occuring within a few hours are assumed to stem from stellar origin, see below. Quantitatively we define the amplitude of the nightly RV variations as "in-night" RV amplitude for a given object. We then computed the following quantities: R_{2d} = (observed RV amplitude – "in-night" RV amplitude)/2 $\times K_{2d}$ and R_{200d} = (observed RV amplitude – "in-night" RV amplitude)/2 $\times K_{200d}$, to be used

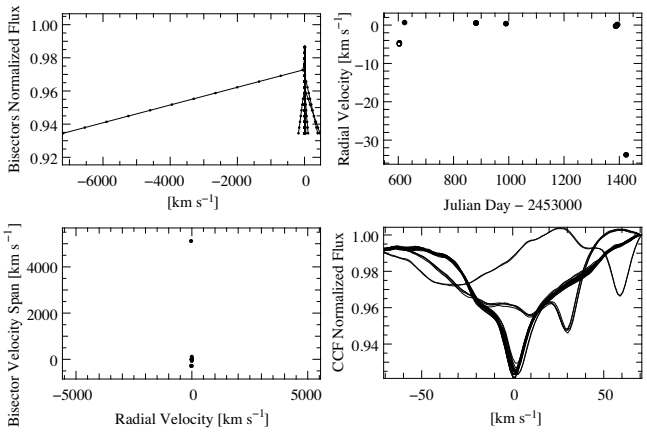

Fig. 2. Example of an SB2 binary, HD 2885 (A2V; $v \sin i = 40$ km s^{-1}). RV curve (*upper right*), CCFs (*lower right*), bisectors (*upper left*), and bisector velocity span (*lower left*). The CCF is clearly variable and indicative of an SB2 binary.

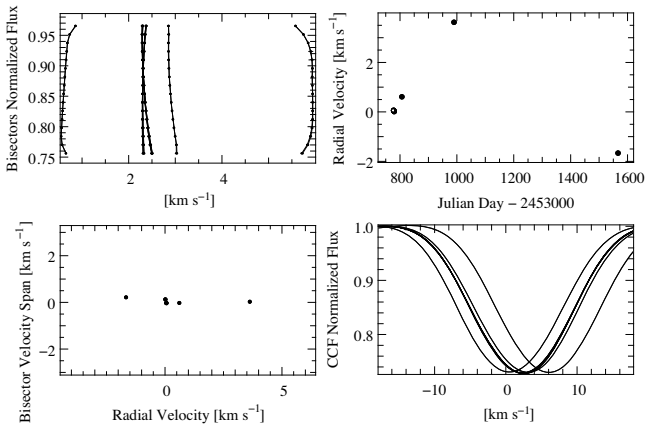

Fig. 3. Example of a binary identified by a flat bisector velocity-span diagram and large amplitude RV variations, HD 68456 (F5V; $v \sin i = 12$ km s^{-1}). RV curve (*upper right*), CCFs (*lower right*), bisectors (*upper left*), and bisector velocity span (*lower left*). The mass of the companion falls in the stellar domain (see text).

as thresholds identifying the binaries. We chose 2 and 200-day periods as they are quite relevant given our temporal sampling and our average time baseline.

For those variable stars for which we could compute a CCF and test the relation between bisectors velocity-span and RV variations, we selected those that show a simple, flat bisector velocity span, i.e., values of bisectors velocity-span arranged horizontally in a (RV; bisector velocity-span) diagram (this corresponds to stars for which the ratio of the amplitude of the bisector velocity span to the RV amplitude is less than 0.2) and for which $R_{2d} \geq 2$ or $R_{200d} \geq 2$. We regard them as unambiguous binaries. Figure 3 provides an example of a variable star (HD 68456; F5V; $v \sin i = 12$ km s^{-1}) for which the bisector velocity span clearly indicates the presence of a companion, and the observed RV amplitude once corrected from in-night variations can be due to a $\simeq 0.1\ M_{\odot}$ stellar companion (see below). This star was also recently classified as a binary on the basis of astrometric data (see below; Goldin & Makarov 2007).

Some variable stars show a bisector velocity span that is either partly flat and partly vertical or partly flat and partly inclined, indicating that they are most probably binaries and at the same time pulsating or active (see below). We classify those objects with R_{2d} or $R_{200d} \geq 2$ as strong binaries candidates. An example, HD 19545 (A3V; $v \sin i = 80$ km s^{-1}), is provided in Fig. 4. Figure 5 compares the case of a pulsating star for which we artificially simulated an additional companion star. The generated RV and span curves of the pulsating star and pulsating star plus stellar companion are comparable to those found in the case of HD 19545. We do not have quantitative criteria to identify those "composite bisectors velocity spans", which explains why we classify the candidates as strong candidates rather than unambiguous binaries.

Finally, for the rest of the stars, we flagged those stars with R_{2d} or $R_{200d} \geq 4$ as binary candidates. For these stars we conservatively adopted a more stringent threshold for R_{2d} or R_{200d} as we lack any additional indication of companions, and we know that these stars may be intrinsically variable. We thus took into account that the actual amplitude RV variations due to the pulsations may be stronger than the one measured on our set of data. This ensures that most of the observed RV amplitudes are due to a perturbation by a BD or a star. Figure 6 gives an example of such a star where no CCF could be computed, and the binarity classification relies solely upon the RV curve.

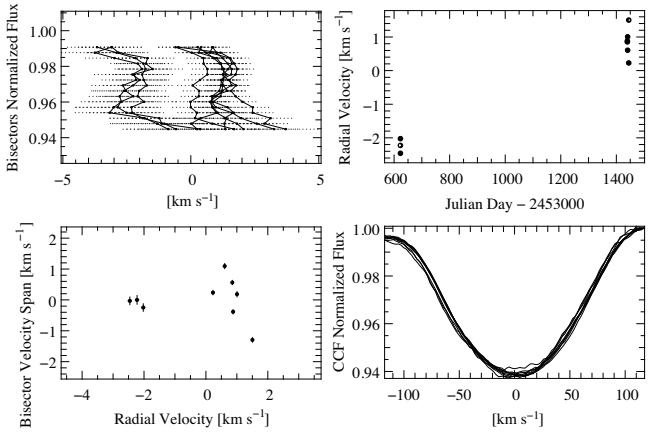

Fig. 4. Example of a star whose RV variations are most probably due to both pulsations and binarity, HD 19545 (A3V; $v \sin i = 80$ km s^{-1}). RV curve (*upper right*), CCFs (*lower right*), bisectors (*upper left*), and bisector velocity span (*lower left*). The CCFs are clearly variable; the bisector velocity-span diagram is composite: part of the data are spread horizontally over a wide velocity range, and part are spread vertically, over a wide range of span. The points that give the vertical bisector velocity span are those associated to the nightly high-frequency RV variations; their bisectors are strongly variable in shape. The points with the low RV are associated to bisector velocity spans that are clearly shifted from the ones corresponding to higher velocities, which produces a shifted bisectors velocity-span.

2.4.2. Planets

Those stars that at the same time show signs of RV variability with low amplitudes and a flat bisector velocity span diagram are very good candidates for hosting planets. In some cases, stars showing composite bisector velocity span diagrams with R_{2d} or R_{200d} larger than 2 can still be "proper" candidates for hosting planets. In such cases, the total RV amplitude is not dominated by the planetary signatures but by stellar variability (e.g., spots).

2.4.3. Intrinsically variable stars

In the case of spots, and provided the star $v \sin i$ is higher than the instrumental resolution, the bisector shape is very peculiar and the bisector velocity-span variations are correlated to the

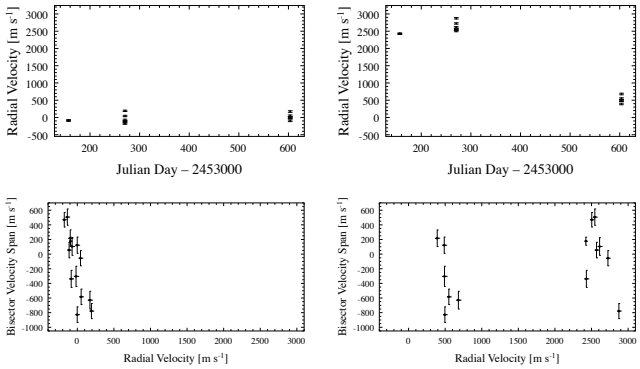

Fig. 5. Simulation of a composite bisector velocity-span diagram produced when adding a 100-$M_{\rm Jup}$ companion on a circular orbit, with a 120-day period around a 1.8-$M_{\odot}$ pulsating star, HD 159492 (A7V; $v \sin i$ = 60 km s^{-1}). The initial RV and bisector velocity-span data are shown on *the left*, where we see in particular high frequency (nightly) RV variations and bisector velocity-spans spread vertically. The simulated data are shown on *the right*. The bisector velocity-span diagram on the right is clearly composite: both flat over a wide range of RV + vertical over a wide range of bisector velocity-span values, similarly to HD 19545.

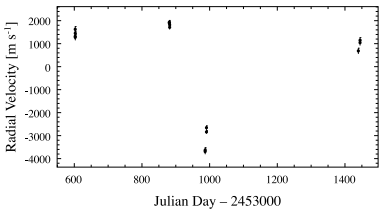

Fig. 6. Example of a star whose RV variations are most probably due to binarity, HD 200761 (A1V; $v \sin i$ = 80 km s^{-1}). RV curve.

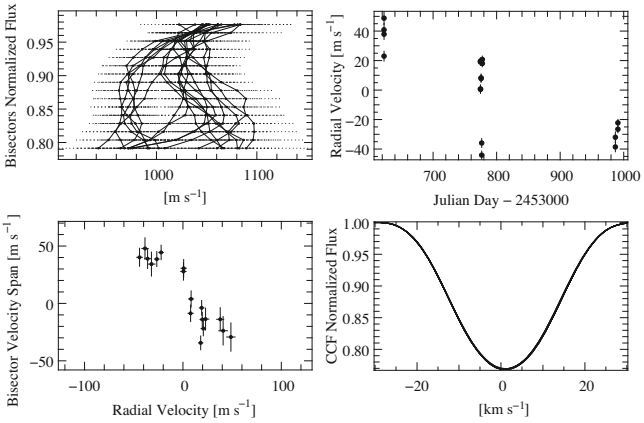

Fig. 7. Example of a star with variable RV due to the presence of spots. HD 25457 (F5V; $v \sin i$ = 25 km s^{-1}). RV curve (*upper right*), CCFs (*lower right*), bisectors (*upper left*), and bisector velocity span (*lower left*).

RV ones (see Desort et al. 2007). In a (RV; bisector velocity span) diagram, the bisector velocity-span values are arranged either as an inclined "8" shape, or along an inclined line (so called "anti-correlation"). For these objects, the ratio of the bisector span amplitude to the RV amplitude is found to be in the range 1–3. Figure 7 provides an example of a star showing clear signatures of spots on the basis of the bisector velocity-span diagram (HD 25457; F5V; $v \sin i$ = 25 km s^{-1}). As another example, the very neat case of HD 138763 can also be found in Desort et al. (2007).

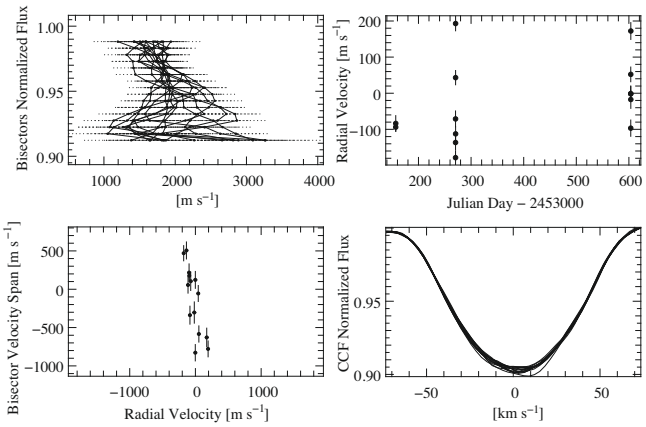

Fig. 8. Example of a star with variable RV due to pulsations. HD 159492 (A7V; $v \sin i$ = 60 km s^{-1}). RV curve (*upper right*), CCFs (*lower right*), bisectors (*upper left*), and bisectors velocity-span (*lower left*).

In the case of pulsations, the bisector velocity-span values are spread over a much wider range than the RV and their variations are not correlated to the RV ones. In a (RV; bisector velocity span) diagram, the bisector velocity-span values are spread vertically, and the ratio of the bisector span amplitude to the RV amplitude is large, typically ≥3. Figure 8 provides an example of a pulsating star (HD 159492; A7V; $v \sin i$ = 60 km s^{-1}).

3. Results

Given the variability criteria described above, 108 stars out of 170 are found to be variable in RV, and 62 are found to be constant in RV within our precision limits. Table 1 provides relevant measurements on these targets: RV amplitudes and uncertainties, bisector velocity-span rms and uncertainties.

3.1. Variability classification

3.1.1. Stellar binaries

Twenty stars are identified as binaries or candidate binaries with the criteria given in the previous section. More precisely:

- 4 binaries are found on the basis of the χ^2 criterium, namely HD 99453, HD 209819, HD 2885 (Fig. 2), HD 142629.
- 6 stars show mostly flat bisector velocity span in a (RV; bisector velocity span) diagram: HD 11262, HD 68456, HD 41742, HD 116568, HD 216627, HD 54834. Their RV amplitude varies between 1600 and 9200 m s^{-1}.
- 4 stars have composite, flat+vertical bisector velocity span in a (RV; bisector velocity span) diagram, together with a total RV amplitude dominated by the binarity effect. These pulsating binaries are: HD 220729, HD 12311, HD 19545 (Fig. 4), and HD 112934.
- Finally, 6 stars are classified as probable binaries solely on the basis of their RV variations: HD 158352, HD 177756, HD 158094, HD 2834, HD 200761 (Fig. 6), HD 116160.

These stars are flagged in Table 1, and an indication of the criteria used to identify them as binaries or possible binaries is also given. No attempt was made to further characterize the stellar companion once the binary status was established, and no more data were recorded on the objects. Their RV variations are given in Fig. 9.

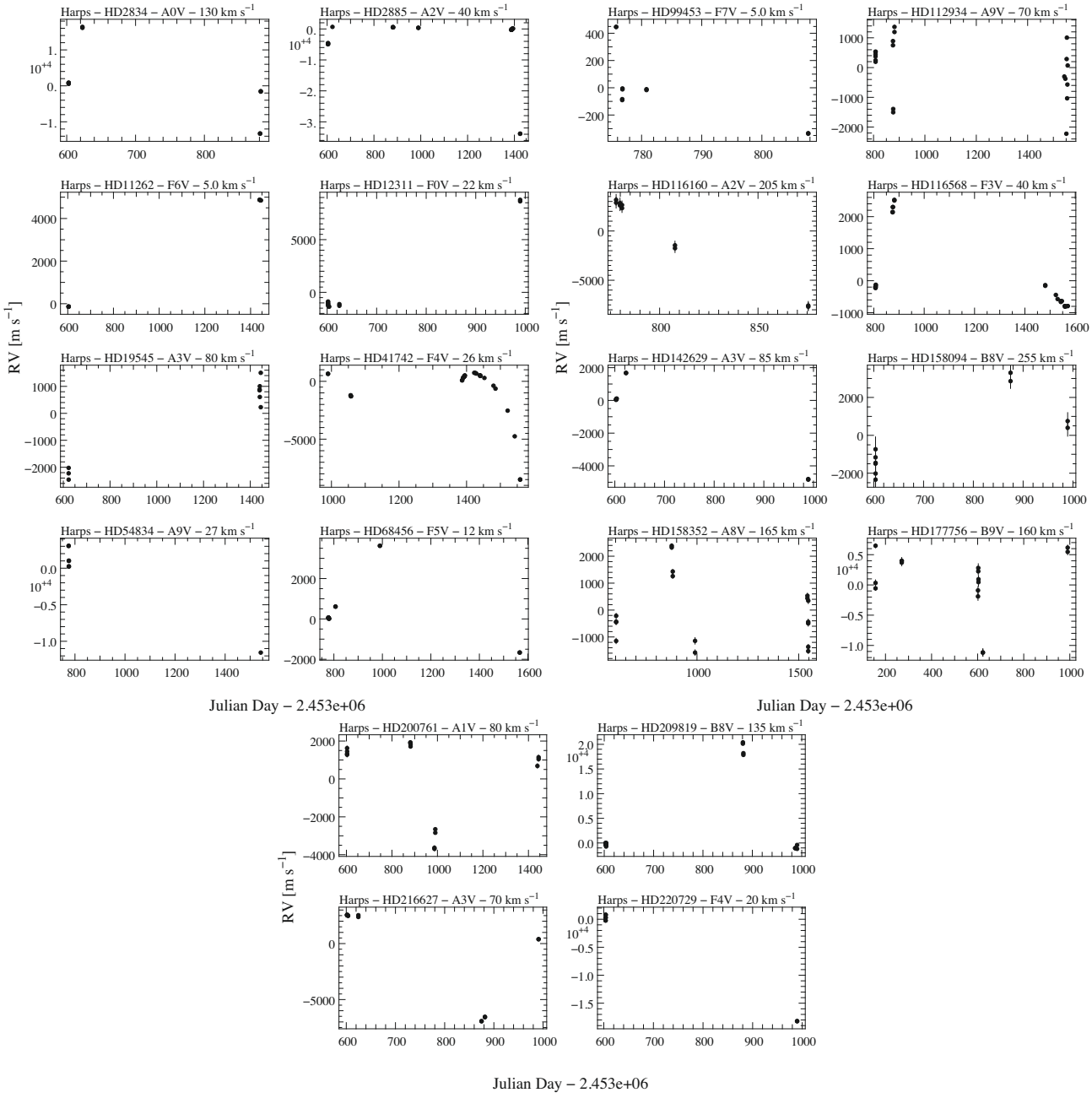

Fig. 9. Radial velocity curves of the identified or strong candidates or probable binaries (see text).

Notes follow on some individual binaries (and potential binaries):

- HD 11262 is associated to a ROSAT source by Suchkov et al. (2003).
- HD 54834: Koen & Eyer (2002) reported this star as a photometric Hipparcos variable at a level of 0.0046 mag and with a frequency of 0.802 day^{-1}. Our data do not either confirm or deny this frequency (not enough points, sampling not adapted).
- HD 68456 (Fig. 3) was not reported as binary in the Hipparcos catalog from the photometric and astrometric points of view; it is classified by Adelman (2001) as one of the least variable Hipparcos stars. Goldin & Makarov (2007), however, provide an orbital solution to fit the Hipparcos astrometric data. The period found is 483 ± 20 days, a_0 = $9.6^{+2.6}_{-1.2}$ mas, eccentricity = $0.12^{+0.25}_{-0.15}$, inclination = 131 ± 16°, $\omega = 103^{+72}_{-68}{}^{\circ}$ and $\Omega = 171^{+164}_{-83}{}^{\circ}$. When fixing the period and eccentricity proposed by these authors, we tried to find a fit to our RV data. They happen to provide good fits assuming a mass of $\simeq 100 M_{\rm Jup}$ for the companion.
- HD 99453: Baade & Kjeldsen (1997) questioned the previously suggested SB2 status of this object on the basis of their data; we do confirm the SB2 status for this star.
- HD 112934 (A9V; $v \sin i = 70$ km s^{-1}): using Hipparcos photometry, Handler (1999) reports this star as a new possible γ Doradus candidate but with a "weak complicated signal", associated to a 0.8-day period, and deCat et al. (2006) did not find clear line-profile variations in their CORALIE data. From our data, the star is both pulsating and a member of a binary system, which makes the line-profile variations indeed more complicated than for pulsating stars. Our limited number of data does not permit the high-frequency period to be characterized.

– HD 116160 was reported as an astrometric binary with accelerating proper motion by Makarov & Kaplan (2005).
– HD 116568 was classified as one of the least variable stars with Hipparcos by Adelman (2001). Baade & Kjeldsen (1997) report no variations in their ±0.5 km s^{-1} spectroscopic survey. The present data show that this star is a binary with an amplitude of at least 2750 m s^{-1}. It is also reported as an unresolved Hipparcos problem star by Masson et al. (1999) and associated to a ROSAT source by Suchkov et al. (2003).
– HD 142629 is an astrometric Hipparcos binary. It was also recently reported for the first time as a spectroscopic binary by Antonello et al. (2006).
– HD 158352 was classified as a possible Herbig AeBe star by The et al. (1994). Corporon & Lagrange (1999) did not find variations to a 5−10 km s^{-1} level in a survey of RV variations among Herbig AeBe stars. This star was reported as being surrounded by a dusty disk by Oudmaijer et al. (1992), and Moor et al. (2006) give an age of 750 ± 150 Myr for the system.
– HD 177756 was classified as a possible λ Bootis star, as well as a possible SB (Farragiana et al. 2004; Gerbaldi et al. 2003). It is reported as one of the Hipparcos least variable stars (Adelman 2001).
– HD 200761 was reported as one of the Hipparcos least variable stars (Adelman 2001).
– HD 209819 was also reported as one of the Hipparcos least variable stars (Adelman 2001).
– HD 220729 is associated to a ROSAT source by Suchkov et al. (2003).

3.1.2. Stars with planets

One star, HD60532 (F6IV–V; $B-V = 0.52$) clearly reveals low-amplitude RV variations and a flat bisector velocity span diagram at the same time, indicative of two Jupiter mass companions with a high confidence level. This star and the results of the fits of the RV curve is presented in Desort et al. (2008). Interestingly, in the frame of the present paper, the periods of the detected planets are long (≥100 days); hence, we get at least 1% of F stars with long-period planets in our sample. This is much less than the predicted rate of ≃10% for 1.5 $M_\odot$ stars by Kennedy & Kenyon (2008); however, we are yet not sensitive to all ranges of masses and periods as shown in the last section.

3.1.3. Single stars: intrinsic variability

We report in Table 1 the RV rms values obtained for each star, together with the associated uncertainties. For all the stars except those identified as binaries, Fig. 10 provides the measured RV rms as a function of their $B-V$, the ratio RV rms/uncertainties (E/I) as a function of their $B-V$ as well, and the ($B-V$; $v \sin i$) diagram for the same objects. In the plots we have distinguished the 88 stars that are found to be variable according to the criteria defined above and those 62 found to be constant according to the same criteria.

The E/I ratio varies between 1.5 and a few tens. It is relatively less for stars with small $B-V$ than for those with larger $B-V$. More quantitatively, the median value for this ratio computed on variable stars is 2.7 (resp. 4.4 and 5.2) for stars with $B-V \leq 0.2$ (resp. $0.2 \leq B-V \leq 0.4$ and $B-V \geq 0.4$). Hence we detect more variable stars among stars with large $B-V$ than stars with smaller $B-V$. We see, moreover, that the uncertainties generally

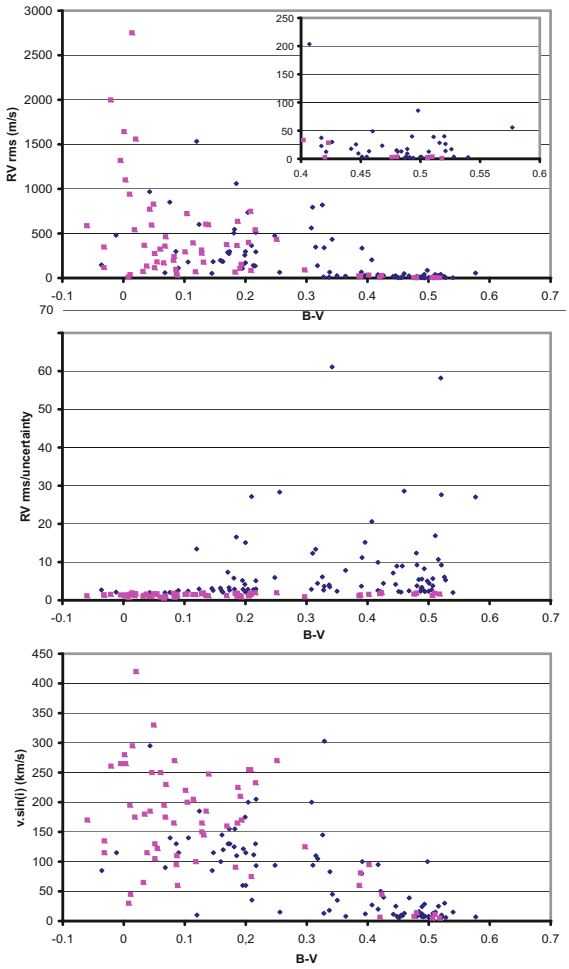

Fig. 10. *Top*: RV rms measured for all stars but binaries with more than 6 spectra available as a function of $B-V$. *Middle*: Ratio RV rms/uncertainty for the same stars. *Bottom*: ($B-V$; $v \sin i$) diagram for the same stars. Losanges indicate RV variable stars and squares indicate RV constant stars.

increase with decreasing $B-V$. These results are not surprising and illustrate that it is more difficult to identify variable stars when they have large uncertainties. In the frame of this study, it is important to keep in mind that our ability to detect variability generally decreases with decreasing $B-V$.

The uncertainties increase with increasing $v \sin i$. We could actually verify that the uncertainties vary as $v \sin i$ with a $(v \sin i)^\alpha$ law where $\alpha = 1.5 \pm 0.1$, as predicted in Galland et al. (2005a). The percentage of variable stars depends on $B-V$ in the following way:

– Most (85%) of the 58 stars with $B-V$ greater than 0.4 are found to be variable and the RV uncertainty is 2 m s^{-1} (median value). Even more, 90% of the 46 stars with $B-V$ over 0.45, i.e., well beyond the instability strip, are found to be variable and their uncertainty is 1.4 m s^{-1} (median value). We conclude then that at a level of precision of 2 m s^{-1} or less, most of the stars with $B-V$ larger than 0.4 are RV variable.
– Among the stars with $B-V$ between 0.2 and 0.4, we found few variable stars, but this is due to a selection effect after known δ Scuti and γ Doradus stars were removed from our sample (see above).
– Only 36% of the 73 stars with $B-V$ less than 0.2 are found to be variable. The percentage of variable decreases to 20%

Table 2. Median values of RV rms and RV uncertainties for stars with more than 6 spectra (3 epochs) available.

$B-V$	[−0.1; 0]	[0; 0.1]	[0.1; 0.2]	[0.2; 0.3]	[0.3; 0.4]	[0.4; 0.5]	[0.5; 0.6]
Number of stars	7	31	32	16	17	30	17
Median RV rms ($m\,s^{-1}$)	480	298	283	330	66	13	4
Median RV uncertainty ($m\,s^{-1}$)	239	300	90	80	19	2	1.4
Median detection limit (P = 3 days)	10	5	4.5	5	0.8	0.17	0.05
Median detection limit (P = 10 days)	15	8	7	7	1.3	0.25	0.08
Median detection limit (P = 100 days)	31	17	15	16	2.8	0.55	0.17
Percentage (3 days)	71	71	94	100	100	100	100
Percentage (10 days)	43	68	78	88	88	100	100
Percentage (100 days)	28	42	44	37	60	100	100

if we consider the 40 stars with $B-V$ under 0.1. For those stars with $B-V$ between 0.1 and 0.2, we get as many variable stars as constant ones. The number of stars found to be constant according to our criteria increases then with decreasing $B-V$. However, we have seen that our ability to detect variable stars decreases with decreasing $B-V$. More quantitatively, the median uncertainty in the case of "constant" stars is $\simeq$290 $m\,s^{-1}$, whereas the median uncertainty in the case of stars found to be variable is $\simeq$80 $m\,s^{-1}$. Furthermore, the median uncertainty of constant stars is comparable to the median value of the standard deviation of variable stars (265 $m\,s^{-1}$). We may then stipulate that, in fact, most of the stars with $B-V \leq 0.2$ are probably RV variable.

When the CCF and bisector velocity-span criteria apply (in fact, whenever the bisector velocity span can be measured with a good or acceptable quality), we may try to characterize the stellar variability further. We find that, as expected in such cases, most of the variable stars with $B-V$ under 0.3 show signs of pulsations, whereas most of the variable stars with greater $B-V$ show signs of spots.

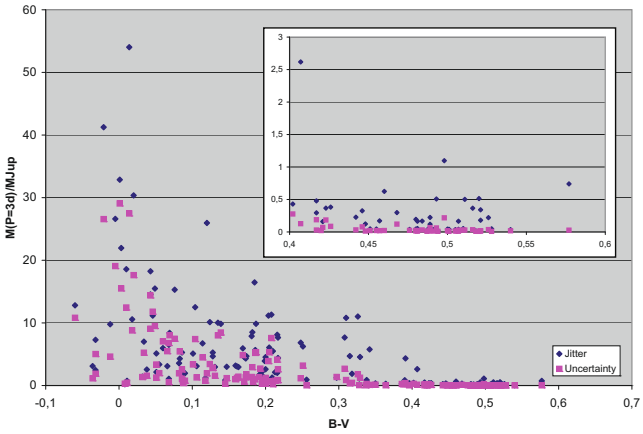

Fig. 11. Achievable detection limits for all stars but binaries taking their actual "uncorrected" jitter (losanges) or the measured uncertainties (squares) into account, and assuming a planet on a circular 3-day orbit.

3.2. Variability of stellar origin and impact on planet detectability

The "uncorrected" jitters, as given directly by the measured RV rms are provided in Table 1 for each star, together with the associated uncertainties. We prefer not to use the jitters corrected from the uncertainties, as sometimes done, as our main aim is to evaluate the impact on planet detectabiliity rather than to make stellar studies. Table 2 gives the computed median "uncorrected" jitters per bins of $B-V$. Rows 7–9 give the median per bin of $B-V$ of the *achievable* detection limits deduced from the measured rms for each star, expressed in Jupiter mass. Three periods are considered: 3, 10 and 100 days (see Sect. 3). We assumed that the planet, supposedly on a circular orbit, is detectable if the amplitude ($2 \times K$) of the RV variations is larger than $3 \times$ RV rms, where RV rms is the "uncorrected" jitter actually measured. We will come back later to a validation of this assumption. Rows 7–9 give the percentage of stars for which the detection limit, given the measured RV rms, fall in the planetary domain.

In Galland et al. (2005a) we showed that the detection limit strongly depends on the star ST and its projected rotational-velocity; more precisely, the detection limit increases with earlier ST and/or larger $v \sin i$. Thanks to the present data, we can in addition address the question of the impact of the stellar jitter.

We give for each star in Table 3 the computed detectable limits assuming 3-day, 10-day, and 100-day periods. Figure 11 shows the detection limits for all stars for a 3-day period. For comparison, we also give the mass of the planet that would be detectable if the star is not active/pulsating (hence has no jitter), and the limit would then be set by the uncertainty (hypothesis $2K = 3\times$ uncertainty). The ratio of the two values is E/I. As previously seen, this ratio is larger than 1.5 and may be quite high; the impact of the jitter on the detectable masses is therefore non negligible. Several comments can be made.

- The achievable limits fall into the planetary domain for a large number of stars: more precisely, in 137 out of 150 stars, i.e., 91%, the detection limit for a 3-day period falls within the planetary domain. For the remaining, stars the limit falls well within the BD domain with masses up to 54 $M_{\rm Jup}$. When considering a 10-day (resp. 100-day) period, we find that we can reach the planetary mass domain for 124 stars, hence 83% (resp. 92 stars, hence 61%). For a 10-day period, the limit for all remaining stars but one fall into the BD regime; for the 100-day period, the limit for all remaining stars but 6 fall in the BD domain.
- As expected, the median of the detection limits *generally* improve with increasing $B-V$, from 10 $M_{\rm Jup}$ for $B-V$ between −0.1 and 0, to 5 $M_{\rm Jup}$ for $B-V$ between 0 and 0.3, to 0.05 $M_{\rm Jup}$ for $B-V$ between 0.5 and 0.6 (for a 3-day period) (see Table 2). Noticeably, for stars with $B-V \geq 0.3$, individual detection limits may be as low as 0.02 $M_{\rm Jup}$ and for stars with $B-V \leq$, 0.3, individual detection limits may be as low as 0.5 $M_{\rm Jup}$. For a ten-day period, these numbers become respectively: 15, 7 and 0.08 $M_{\rm Jup}$; for a 100-day period, 31, 16, and 0.17 $M_{\rm Jup}$. Also, noticeably, the detection limits improve steeply at $B-V = 0.3$.

Table 3. Detection limits, either achievable or achieved with a 68.2% or a 99.7% probability in the present survey (see text); only those detection limits less than 0.05 Jupiter mass are given with 2 digits.

HD	Achievable P = 3 days ($M_{\rm Jup}$)	Achieved P = 3 days ($M_{\rm Jup}$) P = 68.2%	Achieved P = 3 days ($M_{\rm Jup}$) P = 99.7%	Achievable P = 10 days ($M_{\rm Jup}$)	Achieved P = 10 days ($M_{\rm Jup}$) P = 68.2%	Achieved P = 10 days ($M_{\rm Jup}$) P = 99.7%	Achievable P = 100 days ($M_{\rm Jup}$)	Achieved P = 100 days ($M_{\rm Jup}$) P = 68.2%	Achieved P = 100 days ($M_{\rm Jup}$) P = 99.7%
693	0.02			0.04			0.1		
2696	4.7			7.0			15.0		
2834									
2884	13.8	16.8	36.0	20.4	22.4	27.1	44.4	100.0	100.0
2885									
3003	2.7	3.2	6.3	4.1	5.8	12.5	8.8	25.6	100.0
4247	0.4	0.5	1.0	0.6	0.9	1.8	1.2	2.0	6.3
4293	1.4	1.5	1.7	2.0	3.9	49.3	4.4	6.5	33.8
7439	0.1			0.2			0.4		
9672	3.1			4.6			9.9		
11262									
12311									
13555	0.2	0.2	0.4	0.3	0.5	8.2	0.6	3.4	100.0
14943	2.3	2.2	2.4	3.4	3.5	4.7	7.3	8.4	10.8
15008	7.5	9.2	15.2	11.2	14.8	36.2	24.3	32.2	91.4
17848	5.5	6.2	7.3	8.1	10.5	21.8	17.5	25.7	100.0
18978	3.1	6.4	10.6	4.7	9.1	62.9	10.1	21.3	44.4
19107	2.4			3.5			7.6		
19545									
21882	6.1			9.1			19.5		
25457	0.4	0.4	0.4	0.5	0.6	0.6	1.2	2.1	31.8
25490	1.4			2.1			4.6		
29488	3.2	3.1	3.2	4.7	4.9	5.1	10.3	10.3	11.6
29875	5.8			8.6			18.6		
29992	4.7	9.2	100.0	7.0	12.5	100.0	15.2	21.8	48.4
30652	0.2	0.2	0.2	0.3	0.3	0.4	0.6	0.9	2.1
30739	20.0	23.2	44.9	29.6	44.9	94.2	64.4	81.9	100.0
31746	0.2	0.3	0.3	0.4	0.4	0.5	0.8	1.1	2.4
32743	0.2	0.2	0.2	0.3	0.4	1.2	0.6	1.1	100.0
32977	1.3	1.3	2.1	1.9	2.0	2.8	4.1	5.4	14.1
33256	0.05	0.1	0.1	0.1	0.1	0.2	0.2	0.4	100.0
33262	0.2	0.2	0.3	0.3	0.5	1.2	0.7	1.0	1.8
37306	5.5	5.3	6.4	8.1	8.4	9.0	17.7	21.9	46.8
38393	0.1	0.1	0.1	0.1	0.1	0.1	0.2	0.2	0.2
38678	13.4	13.2	16.8	19.8	21.9	29.3	43.0	57.5	97.6
39014	8.2	8.3	10.1	12.1	14.7	22.1	26.4	27.1	27.9
39060	4.5	4.4	4.7	6.6	7.7	9.2	14.4	17.3	29.3
40136	0.1	0.2	0.2	0.2	0.3	0.6	0.5	0.5	0.6
41695	11.2			16.7			35.9		
41742									
43940	10.5	16.9	100.0	15.6	16.5	26.6	33.8	67.2	100.0
46089	16.5			24.6			53.0		
49095	0.04	0.04	0.04	0.1	0.1	0.1	0.1	0.2	0.3
49933	0.4			0.6			1.2		
50445	1.1	1.1	1.5	1.6	1.8	2.1	3.5	3.7	4.1
54834									
56537	3.3	3.9	5.3	4.9	5.9	7.8	10.6	14.8	29.5
59984	0.05	0.1	0.3	0.1	0.1	3.5	0.1	0.3	100.0
60532	0.4	0.4	0.4	0.6	0.6	0.7	1.3	1.4	1.9
60584	0.3	0.3	0.4	0.5	0.6	0.8	1.0	1.9	4.0
63847	11.8	11.9	12.8	17.4	23.0	51.7	37.8	49.2	88.1
66664	11.4	11.6	16.1	16.9	19.8	25.6	36.6	75.4	100.0
68146	0.1	0.1	0.1	0.1	0.1	0.1	0.2	0.2	0.2
68456									
71155	10.5	10.5	11.4	15.6	17.4	21.0	33.9	53.0	100.0
73262	22.0			32.8			70.7		
74591	2.8	2.9	3.1	4.1	4.4	4.8	8.9	14.1	34.0
74873	26.0			38.8			83.5		
75171	4.4			6.6			14.1		
76653	0.2	0.2	0.3	0.3	0.3	0.8	0.6	1.0	1.6
77370	0.5	0.6	0.7	0.8	1.1	2.8	1.7	2.2	5.2

Table 3. continued.

HD	Achievable P = 3 days (M_{Jup})	Achieved P = 3 days (M_{Jup}) P = 68.2%	Achieved P = 3 days (M_{Jup}) P = 99.7%	Achievable P = 10 days (M_{Jup})	Achieved P = 10 days (M_{Jup}) P = 68.2%	Achieved P = 10 days (M_{Jup}) P = 99.7%	Achievable P = 100 days (M_{Jup})	Achieved P = 100 days (M_{Jup}) P = 68.2%	Achieved P = 100 days (M_{Jup}) P = 99.7%
82165	8.7	18.7	100.0	12.9	14.5	17.6	27.9	71.1	100.0
83446	4.6	6.0	16.3	6.8	6.8	7.6	14.8	20.1	48.1
88955	2.3	2.3	2.3	3.4	4.9	10.0	7.4	18.8	100.0
89328	5.0	5.2	6.3	7.4	10.2	39.9	16.0	18.8	32.5
90132	6.7	11.4	100.0	10.0	18.7	100.0	21.6	71.1	100.0
91324	0.04	0.05	0.1	0.1	0.1	0.1	0.1	0.2	0.5
91889	0.1	0.1	0.1	0.1	0.1	0.3	0.2	0.2	0.4
93372	0.1	0.1	0.2	0.1	0.1	0.8	0.2	0.2	0.2
94388	0.2	0.2	0.2	0.3	0.6	1.6	0.7	1.7	100.0
96819	8.4			12.5			27.0		
97244	1.4	1.6	2.2	2.0	2.1	2.7	4.4	12.0	100.0
97603	5.6	8.0	32.8	8.3	11.1	20.0	18.1	41.2	100.0
99211	2.2	3.5	15.5	3.2	6.6	100.0	7.0	19.9	100.0
99453									
100563	0.04			0.1			0.1		
101198	0.5	0.5	0.6	0.8	0.9	1.7	1.7	2.6	20.3
102124	5.0	10.2	100.0	7.4	18.3	100.0	16.1	52.4	100.0
102647	2.1	2.1	2.6	3.1	3.3	4.2	6.7	18.1	100.0
104731	0.3	0.7	9.5	0.5	1.2	100.0	1.0	3.5	100.0
105850	3.6	4.0	6.3	5.3	8.5	100.0	11.6	29.2	100.0
106661	7.0	7.4	19.7	10.4	26.0	100.0	22.5	39.9	100.0
109085	0.3	0.3	0.4	0.4	0.6	6.1	1.0	1.1	2.1
109787	16.6	26.9	100.0	24.7	51.9	100.0	53.5	100.0	100.0
110411	16.4	18.4	21.4	24.3	34.0	54.0	52.8	100.0	100.0
111998	0.5	0.6	0.9	0.8	1.3	8.7	1.7	2.0	3.1
112934									
114642	0.7	0.8	2.0	1.0	1.3	1.7	2.1	35.5	100.0
115892	1.1	1.2	1.8	1.7	2.3	3.8	3.7	67.6	100.0
116160									
116568									
118098	7.2	6.7	7.8	10.7	11.6	18.3	23.1	65.4	100.0
124850	0.5	0.6	0.9	0.8	1.0	1.8	1.6	30.2	100.0
125276	0.02	0.03	0.7	0.02	0.03	0.1	0.1	0.1	100.0
126248	10.8	12.0	14.4	16.0	17.3	22.4	34.7	87.7	100.0
128020	0.02	0.03	0.03	0.05	0.1	0.5	0.1	0.1	100.0
128167	0.3	0.3	0.5	0.4	0.5	0.9	1.0	14.4	100.0
128898	0.9			1.4			3.0		
129422	7.7			11.5			24.7		
129926	5.1	6.3	10.1	7.6	10.8	40.2	16.5	38.9	100.0
130109	26.6			39.8			85.6		
132052	1.9			2.8			6.0		
133469	0.2			0.3			0.7		
135379	0.6	1.1	12.1	0.9	1.5	8.2	1.9	2.5	6.9
135559	8.4	8.4	9.2	12.5	13.0	15.9	27.0	70.8	100.0
138763	0.7	0.7	0.8	1.0	1.3	2.0	2.2	3.9	19.8
139211	0.04	0.04	0.05	0.1	0.1	1.7	0.1	0.2	100.0
141513	3.3	3.4	4.1	4.9	6.0	7.8	10.7	25.4	100.0
141851	10.0			15.0			32.3		
142139	0.8			1.2			2.5		
142629									
145689	3.2			4.8			10.2		
146514	11.0			16.5			35.4		
146624	0.2			0.3			0.7		
147449	1.0	1.0	1.1	1.4	1.5	2.0	3.1	6.1	57.2
153363	2.8	3.7	8.9	4.2	16.1	100.0	9.1	13.2	24.9
156751	6.8			10.2			22.0		
158094									
158352									
159170	9.9			14.7			31.7		
159492	1.7	3.4	100.0	2.6	3.8	18.3	5.6	10.7	100.0

Table 3. continued.

HD	Achievable $P = 3$ days ($M_{\rm Jup}$)	Achieved $P = 3$ days ($M_{\rm Jup}$) $P = 68.2\%$	Achieved $P = 3$ days ($M_{\rm Jup}$) $P = 99.7\%$	Achievable $P = 10$ days ($M_{\rm Jup}$)	Achieved $P = 10$ days ($M_{\rm Jup}$) $P = 68.2\%$	Achieved $P = 10$ days ($M_{\rm Jup}$) $P = 99.7\%$	Achievable $P = 100$ days ($M_{\rm Jup}$)	Achieved $P = 100$ days ($M_{\rm Jup}$) $P = 68.2\%$	Achieved $P = 100$ days ($M_{\rm Jup}$) $P = 99.7\%$
160613	1.7			2.6			5.6		
161868	14.5			21.7			46.8		
164259	0.9	1.2	2.4	1.4	2.0	3.6	3.0	4.2	8.2
167468	19.6	23.4	31.6	29.1	46.4	100.0	63.1	83.4	100.0
171834	0.3	0.4	0.5	0.5	0.5	0.7	1.0	2.2	100.0
172555	4.2	5.1	11.3	6.2	7.6	11.3	13.5	20.7	33.0
175638	3.3	3.8	4.7	4.8	5.9	8.0	10.5	17.8	38.3
175639	11.2			16.7			35.9		
176638	41.2			61.6			132.7		
177178	8.5			12.7			27.4		
177724	54.0			80.7			173.9		
177756									
181296	32.7	40.0	76.3	48.4	49.3	68.7	105.2	100.0	100.0
184985	0.04	0.1	0.1	0.1	0.1	0.1	0.1	0.2	0.6
186543	2.5	2.6	3.3	3.6	4.2	6.9	7.9	12.3	43.9
187532	0.5	0.6	1.1	0.7	0.7	0.8	1.5	3.9	10.4
188228	2.6	3.2	6.7	3.9	5.7	72.4	8.5	10.0	17.6
189245	1.1	2.7	100.0	1.7	2.4	10.0	3.6	8.2	100.0
191862	0.04			0.1			0.1		
196385	0.2	0.2	0.4	0.3	0.3	1.1	0.6	1.0	100.0
197692	0.4	0.4	0.5	0.6	0.7	0.7	1.3	9.4	100.0
198390	0.04			0.1			0.1		
199254	3.2	4.7	7.0	4.7	4.9	4.9	10.2	16.9	100.0
199260	0.2	0.2	0.3	0.2	0.3	0.4	0.5	1.2	13.8
200761									
202730	1.7			2.5			5.3		
203608	0.02	0.02	0.03	0.03	0.04	0.1	0.1	0.2	100.0
205289	0.4	0.5	0.8	0.6	0.6	0.8	1.3	6.1	100.0
209819									
210302	0.1	0.1	0.1	0.2	0.2	0.2	0.4	0.6	1.0
210418	5.7	7.0	13.6	8.4	11.9	38.7	18.2	21.4	28.8
210739	5.9			8.9			19.1		
211976	0.1	0.1	100.0	0.1	0.1	0.2	0.2	0.3	100.0
212728	12.4	13.0	15.5	18.3	28.2	60.8	39.8	63.9	100.0
213398	0.8	1.4	8.5	1.2	1.7	5.9	2.6	3.9	9.4
213845	0.3	0.3	0.4	0.5	0.6	0.8	1.1	1.6	3.5
215789	4.6	3.5	100.0	6.8	4.7	7.1	14.8	3.4	100.0
216627									
216956	0.9	3.6	100.0	1.3	3.2	8.1	2.9	10.0	100.0
219482	0.2	0.2	0.4	0.3	0.4	2.6	0.6	0.9	2.4
220729									
222095	3.8	4.1	5.5	5.7	7.6	11.0	12.3	15.9	39.9
222368	0.04	0.05	0.1	0.1	0.1	0.1	0.1	0.1	0.2
222603	4.5			6.8			14.6		
222661	7.3			10.9			23.5		
223011	6.0	6.7	9.6	8.9	13.2	96.8	19.3	30.4	79.8
223352	32.9			49.1			105.8		
223781	5.7			8.5			18.2		
224392	6.0			8.9			19.2		

– The "uncorrected" jitter varies a lot from one object to the next; therefore, the general conclusion that the detection limits improves with increasing $B - V$ may not apply when considering individual objects. For instance, the two stars HD 50445 (A3V; $B - V = 0.18$) and HD 63847 (A9V; $B - V = 0.3$) have similar projected rotational-velocities ($v \sin i \simeq 90$ km s^{-1}) and very different levels of activity, with an RV rms of 66 m s^{-1} and 794 m s^{-1}, respectively. When we take this "uncorrected" jitter into account, the detection limit is 1 $M_{\rm Jup}$ ($P = 3$ days) and 1.5 $M_{\rm Jup}$ ($P = 10$ days) around the A3V star, whereas the detection limit is about 10 times higher for the A9V star.

We conclude then that planets can indeed be found around a wide range of stars with $B - V$ greater than -0.1, even taking their jitter into account. The achievable detection limit of such early type stars cannot be predicted given only the star properties (ST, $v \sin i$), but requires data to be recorded data to estimate their level of jitter.

We note that, of course, the measured "uncorrected" jitter provides a reliable limit to planet detection only when this jitter

is due to stellar activity in general and not to companions. Were a companion present, its contribution to the RV variability would have to be removed in order to estimate the impact of the stellar activity.

4. Planet detection limits of the present survey

4.1. Estimation of the achieved detection limits

We now try to estimate the detection limits reached by the present survey, taking the actual RV curve into account. For each star, we then compute the detection limit (companion mass) as a function of its period. To do so, we consider a planet with a given mass and with a given period (the orbit is assumed to be circular). For any couple (mass; period) we generate a large number of Keplerian orbits, assuming different times of passage at periastron (T_0). For each orbit, we compute the expected radial velocities at the times of the actual observations. We add a noise (random value between $\pm$ RV uncertainty), where RV uncertainty is the uncertainty measured on the RV data. We then get a virtual set of RVs, which takes the star properties into account (in particular, its ST and rotational velocity, through the uncertainties and SN). We then compute the standard deviation of the virtual RVs points. For a given (mass; period), the distribution of all the standard deviations (corresponding to different T_0) obtained is Gaussian. We then compute the average value of the distribution of the virtual standard deviations. We consider that a planet with a given (mass; period) is detectable if the standard deviation of the real RV values is less than the average value of the virtual standard deviations. We determine the confidence level (or detection probability) associated to such an orbit by comparing the standard deviation of the virtual distribution with the difference between the standard deviation of the real RV measurements and the average value of the virtual standard deviations.

In practice, for a given object, we explored 200 periods in the range 0.5 to 1000 days, and 100 planet masses in the range (Mmin; 100 $M_{\rm Jup}$) where Mmin corresponds to the achievable mass given the measured uncertainty. For a given (mass; period), we explored 1000 T_0. We checked that increasing the number of periods, planet masses, and/or initial T_0 do not significantly affect the results.

For each (mass; period) couple, we thus obtain a detection probability. In a (mass; period) diagram, we can then identify the domain where a planet with a given mass and period should be detectable if present, with a given level of confidence. This defines a domain in which we can exclude the presence of a planet with a given level of confidence. We consider two levels of confidence: 1σ (i.e., a 68.2% probability) and 3σ (i.e., 99.7% probability).

4.2. Sensitivity of the survey and first constraints on early type stars

The sensitivity of our survey is a consequence of the number of data available and on the temporal sampling of the data. We kept only those stars (107 objects) found to be either constant or variable, for which we got more than 12 data points (6 epochs). Also, given the data at hand, we limited the range of periods investigated between 1 day and a few hundred days. We report in Table 3 the achieved limits (68.2% and 99.7% probabilities) obtained for each of the 107 stars considering three periods: 3, 10, and 100 days.

We also give in Fig. 12 examples of the detection limits achieved (68.2% and 99.7% probabilities) as estimated with the previously described simulations. We also plotted the achievable detection limits taking the jitter into account, as defined in the previous section, as well as the detection limits corresponding to the measured uncertainties. We recall that the last two cases (achievable limits) do not take the actual temporal sampling of the data into account, conversely to the detection limits computed with our virtual realizations.

When enough data are available, the actual detection limits fall close to the achievable limits obtained assuming the $3 \times$ RV rms threshold for the amplitude of RV variations, as can be seen in Fig. 12. This justifies the choice of the threshold adopted in the previous section to estimate the achievable limits.

We sometimes endup with high detection limits that fall outside the investigated range of masses, i.e., $\geq$100 $M_{\rm Jup}$ when we consider a period of 100 days, whereas the detection limits for a 3- or 10-day period are close to the achievable limits. This corresponds to cases where the temporal sampling is not adapted to exploring such a long period (see for instance the case of HD 33256, in Fig. 12). Sometimes, but much less frequently, the detection limit for a 10-day fall outside the investigated range of masses, whereas the detection limits for a 3-day period is close to the achievable limit. In fact, our survey searches mostly for short-period planets (typ. a few days). Ten to 100-day periods are not always sampled often enough to get interesting results (especially on early-type stars) and $\geq$100-day periods are not properly sampled to get interesting results. We therefore discuss only periods $\leq$100 days. Finally, one has to note that, in some cases, we get a 99.7% probability detection limit out of the investigated range, whereas the 68.2% limit falls well into the investigated range. This happens generally when the number of data is the lowest: 12 or 14.

To study the impact of $B-V$ on the present results, we computed the percentage of stars for which the achieved detection limits (68.2% and 99.7% probabilities) fall in the planetary or BD domains per bin of $B-V$, considering a 3-day, a 10-day, and a 100-day period. We also computed the median of the achieved detection limits (considering 68.2% and 99.7% probabilities) per bin of $B-V$ for such periods. The results are given in Table 4. In order to allow comparison between the limits obtained with these two probabilities and with the achievable ones, we considered only those stars for the computation of the median values for which both the 68.2% and 99.7% probability detection limits fall within the investigated range of masses. Finally, one has to note that, for the earliest type stars, there are few objects per bin is quite small, so one has to be very cautious with the associated statistics. We can see that

- if we consider a 3-day period, the achieved limit at 1σ (resp. 3σ) falls within the planetary domain for 90% (resp. 81%) of the stars. This percentage is comparable to the one found in Sect. 3. It increases from 75% (resp. 25%) for the earliest type stars to 100% (resp. 100%) for stars with $B-V$ greater than 0.3. Also, the median of the achieved limits at 1σ (resp. 3σ) decreases from 7 $M_{\rm Jup}$ (resp. 7 $M_{\rm Jup}$) for the earliest-type stars to 0.08 $M_{\rm Jup}$ (resp. 0.3 $M_{\rm Jup}$) for the latest-type stars. Moreover, the steep step seen in Sect. 3 in the detectable masses at $B-V=0.3$ is also clear.
- if we consider a 10-day period, the achieved limit at 1σ (resp. 3) fall in the planetary domain for 82% (resp. 67%) of the stars. This percentage increases from 50 (resp. 25)% for the earliest type stars to 100% (resp. 100%) for stars with $B-V$ larger than 0.4, however, with an exception in the [0.2; 0.3] range where it decreases back to 50%. Also,

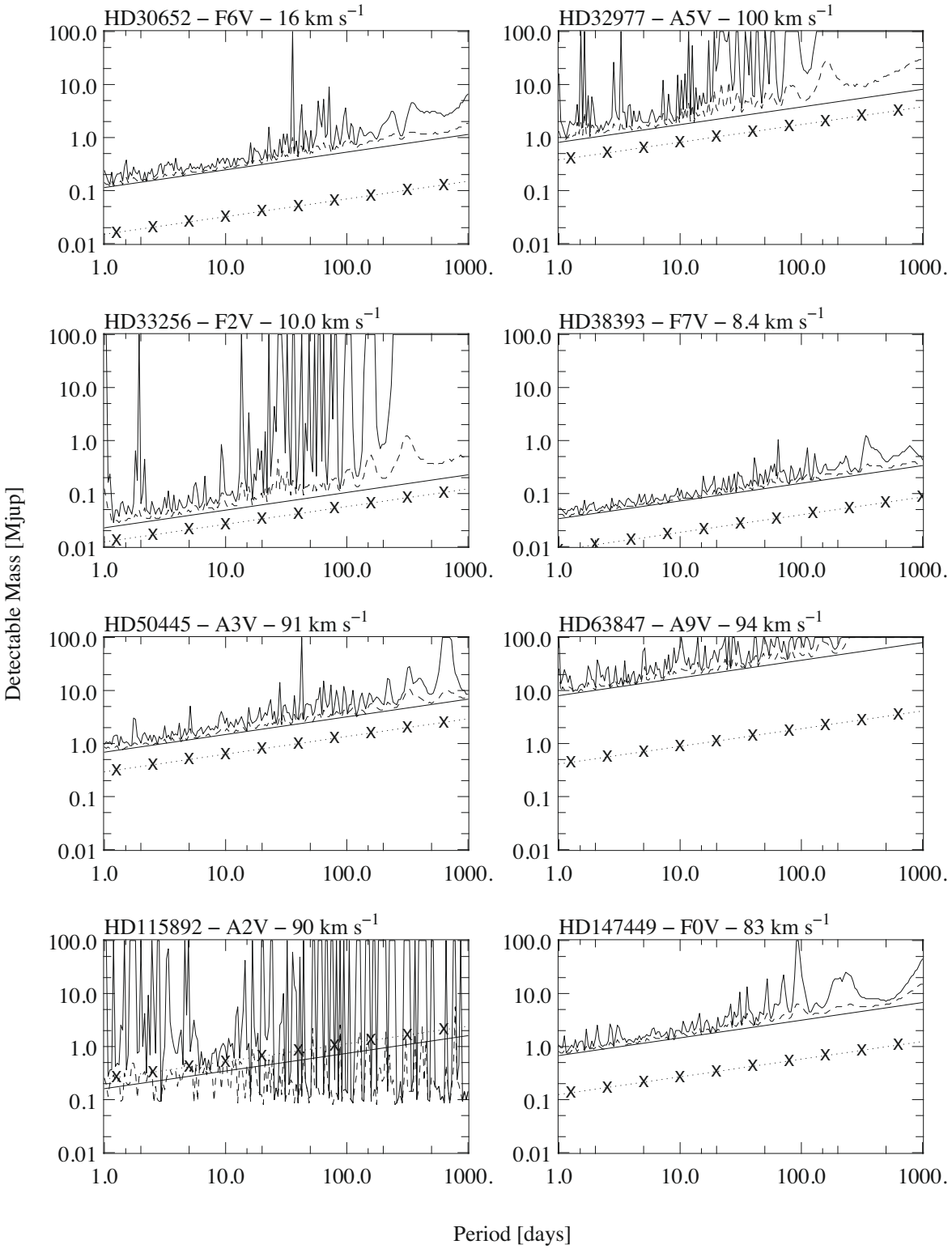

Fig. 12. Detection limits. *X*-axis: periods (days). *Y*-axis: detection limit (M/$M_{\rm Jup}$). Curve: detection limits actually achieved in the present survey; plain curves correspond to 99.7% detection probability, and broken curves to 68.2% probability. The RV data were averaged beforehand over one day. Straight line: achievable detection limits assuming a 3× rms threshold for the planet amplitude. Line with crosses: achievable detection limits assuming a 3× uncertainty threshold for the planet amplitude.

the median of the achieved limits at 1σ (resp. 3σ) decreases from 12 $M_{\rm Jup}$ (resp. 24 $M_{\rm Jup}$) for the earliest-type stars to 0.1 (resp. 0.7) for the latest-type stars, with however an exception in the range [0.2; 0.3] range as regards the 99.7% probability. Again the steep step is observed at $B - V = 0.3$.

– if we finally consider a 100-day period, the achieved limit at 1σ (resp. 3σ) falls within the planetary domain for 54% (resp. 35%) of the stars. We note that this percentage is lower than the one obtained in Sect. 3, so we attribute the discrepancy to the actual temporal sampling and the

Table 4. Percentage of stars for which the achieved detection $P = 68.2\%$ or $P = 99.7\%$ limits fall in the planetary or BD/planet domains. Median values of the *achieved* detection limits, expressed in Jupiter mass, per bin of $B - V$.

$B - V$	[−0.1; 0]	[0; 0.1]	[0.1; 0.2]	[0.2; 0.3]	[0.3; 0.4]	[0.4; 0.5]	[0.5; 0.6]
number of stars (whole sample)	4	19	21	10	12	24	17
$P = 3$ days							
Percentage of limits in the planet domain ($P = 68.2\%$; $P = 99.7\%$)	75; 25	74; 47	95; 61	100; 60	100; 100	100; 100	100; 100
Percentage of limits in the BD/planet domain ($P = 68.2\%$; $P = 99.7\%$)	100; 100	100; 100	100; 100	100; 100	100; 100	100; 100	100; 100
$P = 10$ days							
Percentage of limits in the planet domain ($P = 68.2\%$; $P = 99.7\%$)	50; 25	58; 42	80; 52	50; 30	92; 66	100; 100	100; 100
Percentage of limits in the BD/planet domain ($P = 68.2\%$; $P = 99.7\%$)	100; 100	100; 52	100; 95	100; 64	100; 92	100; 92	100; 100
$P = 100$ days							
Percentage of limits in the planet domain ($P = 68.2\%$; $P = 99.7\%$)	25; 0	16; 10	28; 10	30; 10	58; 33	92; 55	94; 47
Percentage of limits in the BD/planet domain ($P = 68.2\%$; $P = 99.7\%$)	75; 25	74; 83	95; 48	100; 40	100; 58	100; 59	100; 100
$P = 3$ days							
Number of stars	4	17	17	8	11	22	17
Achieved detection limit ($P = 68.2\%$)	6.9	5.3	5.1	3.2	0.5	0.25	0.08
Achieved detection limit ($P = 99.7\%$)	6.9	12.1	7.3	6.3	1.0	0.3	0.3
Achievable detection limit	6.9	5.5	4.2	2.5	0.4	0.2	0.06
$P = 10$ days							
Number of stars	4	14	20	7	11	22	17
Achieved detection limit ($P = 68.2\%$)	11.7	8.0	7.2	4.4	0.9	0.4	0.1
Achieved detection limit ($P = 99.7\%$)	24.0	11.8	10.2	17.4	2.0	0.8	0.7
Achievable detection limit	10.3	6.9	5.6	4.1	0.6	0.3	0.1
$P = 100$ days							
Number of stars	1	6	11	5	8	13	12
Achieved detection limit ($P = 68.2\%$)	(10.0)	18.7	17.3	14.2	5.2	1.1	1.0
Achieved detection limit ($P = 99.7\%$)	(17.6)	34.4	32.9	33.8	20.4	2.4	1.9
Achievable detection limit	(8.5)	15.0	10.5	8.9	3.0	0.8	0.6

relatively small amount of targets investigated yet. The median of the achieved limits at 1σ (resp. 3σ) decreases from 19 $M_{\rm Jup}$ (resp. 34 $M_{\rm Jup}$) for stars with $B - V \geq 0.0$ to 1 $M_{\rm Jup}$ (resp. 1.9 $M_{\rm Jup}$) for the latest-type stars. Again this steep step is observed at $B - V = 0.3$.

Finally, we give the probability of *not* detecting planets of a given mass and with a given period (3, 10, 200, 500 days) around stars with a given spectral type and $v \sin i$. The results are summarized in Table 5. We see that as expected, for a given probability, the limits globally decrease with increasing $B - V$ and decreasing $v \sin i$.

Obviously, the statistics provided by our survey are still poor on early type stars, and still very limited on the latest type stars. Concerning the latter, we note that, if we consider the 41 objects with $B - V \geq 0.4$, i.e., well beyond the instability strip, we find that less than 24% of stars host planets with masses equal to 0.5 $M_{\rm Jup}$ or more; less than 5% host planets with masses equal to 1 $M_{\rm Jup}$ or more on a 3-day period. For a 10-day period, we find that less than 42% host planets with masses ≥0.5 $M_{\rm Jup}$, and less than 20%) host planets with masses ≥1 $M_{\rm Jup}$. The comparison between achieved and achievable detection limits shows that there is still room to significantly improve those statistics (thanks to new data points).

The present statistics certainly do not allow quantitative comparisons with late type dwarfs, which have been surveyed by several groups for more than 10 years, or with giant or subgiant stars, because in that case of the lack of data for both massive dwarfs and (sub-)giants.

Table 5. Detection limit for 50% and 90% for different periods.

ST, $v \sin i$	Period [days]	50% [$M_{\rm Jup}$]	90% [$M_{\rm Jup}$]	N-st.⋆
early A, $v \sin i \leq 70$ km s^{-1}	3	1.2	–	2
	10	1.7	–	2
	200	4.7	–	2
	500	6.4	–	2
early A, $v \sin i$ 70–130 km s^{-1}	3	4.6	7.2	9
	10	6.9	10.7	9
A, $v \sin i \leq 70$ km s^{-1}	3	3.5	–	2
A, $v \sin i$ 70–130 km s^{-1}	3	4.5	6.3	10
	10	6.7	9.5	10
A, $v \sin i \geq 130$ km s^{-1}	3	11.2		13
F, $v \sin i \leq 15$ km s^{-1}	3	0.1	0.8	28
	10	0.2	1.2	28
	200	0.4	3.2	25
	500	0.6	2.7	22
F, $v \sin i$ 15–60 km s^{-1}	3	0.6	0.8	13
	10	0.9	1.2	13
	200	2.8	3.3	12
	500	3.8	4.5	12
F, $v \sin i \geq 60$ km s^{-1}	3	1.9	10.2	10
	10	2.8		10
	200	7.5		9
	500	10.1		9

⋆ Number of stars considered to estimate these detection limits. Note: only stars with more than 12 measurements (6 epochs) were considered, binaries were excluded, and numbers outside the planetary mass domain (>13 $M_{\rm Jup}$) are not given.

Concerning the presence or absence of hot Jupiters around massive stars, we note that the planets found so far in our survey are located at about 0.7 AU or more from a 1.4 $M_{\odot}$ star. This separation corresponds to what is found for the closest planet around giant stars. We have also recently detected a planet orbiting at 0.6 AU from a dwarf with a similar mass in the northern hemisphere (Desort et al. 2009). Because of the still limited amount of data available, it should not, however, be concluded that there are no planets closer to massive dwarfs. We also recall that a few short-period planets have been found around 1.4 $M_{\odot}$ stars through transits.

5. Conclusion

Based on the observation of a large number of A–F type stars (170), we have been able to measure their jitters and, for the first time, derive estimations of the detection limits that can be expected on average on those stars with $B - V$ in that range $[-0.1; 0.6]$ (once previously known δ Scuti and γ Doradus stars are removed) for 3 periods: 3, 10, and 100 days. We have shown that, at the precision provided by HARPS, most of the stars are variable in RV, and the impact of the RV jitter, due to either spots or pulsations, is generally not negligible on planet detectability. However, assuming that planets are detectable if the amplitude of the induced RV variation is greater than 3×rms (this threshold defines the achievable detection limits, which depends on the star and the spectrograph used), we have shown that, even when taking into account the jitter, giant planets can still be found around these stars in most cases. This is not only true for the stars with $B - V \geq 0.3$, for which we can find either short- or long-period planets, with masses as low as 0.02 $M_{\rm Jup}$ (case of short period) for the latest type stars, but also for dwarfs with $B - V \leq 0.3$. For such stars, short-period planets can still be found around those with relatively low projected rotational velocity and low level of activity, with masses down to 0.5 $M_{\rm Jup}$ (best case). This survey has identified for the first time those stars that are best-suited to further searches for planets around massive dwarfs.

We have also shown that, given the data available, the present survey is sensitive to short-period planets (hot Jupiters) and only partially sensitive to longer periods (up to 100 days). We found in particular one 2-planet system with periods longer than 100 days around one late-type star. Whenever possible (107 stars), we computed the detection limits actually achieved for each star and showed that when enough data are available, the achieved detection limit is set by the $3 \times$ rms threshold. We indeed reached such limits for early-type, as well as for late-type stars. We finally derived first estimates of the presence of short-period planets around these A–F stars. We showed for instance that fewer than 5% of the latest-type stars ($B - V \geq 0.4$) host $P = 3$ day-period planets with masses 1 $M_{\rm Jup}$ or more. Such statistics are not constraining enough to allow interesting comparisons with later type stars or with model predictions, but as soon as more data become available, the statistics can be improved straightforwardy.

Finally, we note that to compute these detection limits, we did not try to average out the spectra over timescales associated to the frequencies of intrinsic stellar variations. This approach would of course allow a significant decrease in the detectable masses. As it would require lots of telescope time, it should probably be kept for stars with the highest scientific interest.

Acknowledgements. We acknowledge financial support from the French Programme National de Planétologie (PNP, INSU). We also acknowledge support from the French National Research Agency (ANR) through project grant NT05-4_44463.
These results have made use of the SIMBAD database, operated at the CDS, Strasbourg, France.
We also thank Gérard Zins and Sylvain Cètre for their help in implementing the SAFIR interface, Sylvain Cètre also for performing some of the observations, and P. Rubini for his help on the layout of the paper.

References

Adelman, S. J. 2001, A&A, 367, 297
Antonello, E., Mantegazza, L., Rainer, M., & Miglio, A. 2006, A&A, 445, L15
Baade, D., & Kjeldsen, H. 1997, A&A, 323, 429
Bonfils, X., Forveille, T., Delfosse, X., et al. 2005, A&A, 443, L15
Burkert, A., & Ida, S. 2007, ApJ, 660, 845
Butler, R. P., Johnson, J. A., Marcy, G. W., et al. 2006, PASP, 118, 1685
Corporon, P., & Lagrange, A.-M. 1999, A&A, 136, 429
De Cat, P., Eyer, L., Cuypers, J., et al. 2006, A&A, 449, 281
Desort, M., Lagrange, A.-M., Galland, F., et al. 2007, A&A, 473, 893
Desort, M., Lagrange, A.-M., Galland, F., et al. 2008, A&A, 491, 883
Desort, M., Lagrange, A.-M., Galland, F., et al. 2009, A&A, in preparation
Farragiana, R., & Bonifacio, G. 2004, A&A, 349, 521
Galland, F., Lagrange, A.-M., Udry, S., et al. 2005a, A&A, 443, 337
Galland, F., Lagrange, A.-M., Udry, S., et al. 2005b, A&A, 444, L21
Galland, F., Lagrange, A.-M., Udry, S., et al. 2006, A&A, 452, 709
Gerbaldi, M., Farragiana, R., & Lai, O. 2003, A&A, 412, 447
Goldin, A., & Makarov, V. V. 2007, ApJS, 173, 137
Ida, S., & Lin, D. N. C. 2005, ApJ, 626, 1045
Handler, G. 1999, MNRAS, 309, L19
Hatzes, A. P. 2002, Astron. Nachr., 323, 3/4, 392
Hatzes, A. P., Guenther, E. W., Endl, M., et al. 2005, A&A, 437, 743
Hekker, S., Reffert, S., Quirrenbach, A., et al. 2006, A&A, 454, 943
ESA 1997, The Hipparcos and Tycho Cat, ESA SP-1200
Johnson, J.A., Marcy, G.W., Fisher, D.A., et al. 2006, ApJ, 652, 1724
Johnson, J.A., Butler, R.P., Marcy, G.W., et al. 2007, ApJ, 665, 785
Kennedy, G. M., & Kenyon, S. J. 2008, ApJ, 673, 502
Koen, C., & Eyer, L. 2002, MNRAS, 331, 45
Li, S. L., Lin, D. N. C., & Liu, X. W. 2008, ApJ, 685, 1210
Lovis, C., & Mayor, M. 2007, A&A, 472, 657
Makarov, V. V., & Kaplan, G. H. 2005, AJ, 129, 2420
Masson, B. D., Martin, C., Hartkopf, W. I., et al. 1999, AJ, 117, 1890
Mathias, P., Le Contel, J.-M., & Le Chapellier, E. 2004, A&A, 417, 189
Moor, A., Abraham, P., derekas, A., et al. 2006, ApJ, 644, 525
Niedzielski, A., Konacki, M., Wolszcan, A., et al. 2007, ApJ, 669, 1354
Rodriguez, E., Lopez-Gonzales, M. J., & Lopez de Coca, P. 2000, A&A, 144, 469
Saar, S. H., & Donahue, R. A. 1997, ApJ, 485, 319
Sato, B., Ando, H., Takeda, Y., et al. 2003, ApJ, 597, L157
Sato, B., Izumiura, H., Toyota, E., et al. 2008, PASJ, 60, 539
Suchkov, A. A., Makarov, V. V., & Voges, W. 2003, ApJ, 595, 1206
The, P. S., de Winter, D., & Perez, M. R. 1994, A&AS, 104, 315
Oudmaijer, R. D., et al. 1992, A&AS, 96, 625